

# Jade-1 inhibits Wnt signalling by ubiquitylating $\beta$ -catenin and mediates Wnt pathway inhibition by pVHL

Vipul C. Chitalia<sup>1</sup>, Rebecca L. Foy<sup>1</sup>, Markus M. Bachschmid<sup>2</sup>, Liling Zeng<sup>1</sup>, Maria V. Panchenko<sup>1</sup>, Mina I. Zhou<sup>1</sup>, Ajit Bharti<sup>3</sup>, David C. Seldin<sup>4</sup>, Stewart H. Lecker<sup>5</sup>, Isabel Dominguez<sup>4</sup> and Herbert T. Cohen<sup>1,4</sup>

**The von Hippel–Lindau protein pVHL suppresses renal tumorigenesis in part by promoting the degradation of hypoxia-inducible HIF- $\alpha$  transcription factors<sup>1</sup>; additional mechanisms have been proposed<sup>2</sup>. pVHL also stabilizes the plant homeodomain protein Jade-1, which is a candidate renal tumour suppressor that may correlate with renal cancer risk<sup>3–5</sup>. Here we show that Jade-1 binds the oncoprotein  $\beta$ -catenin in Wnt-responsive fashion. Moreover, Jade-1 destabilizes wild-type  $\beta$ -catenin but not a cancer-causing form of  $\beta$ -catenin. Whereas the well-established  $\beta$ -catenin E3 ubiquitin ligase component  $\beta$ -TrCP ubiquitylates only phosphorylated  $\beta$ -catenin<sup>6</sup>, Jade-1 ubiquitylates both phosphorylated and non-phosphorylated  $\beta$ -catenin and therefore regulates canonical Wnt signalling in both Wnt-off and Wnt-on phases. Thus, the different characteristics of  $\beta$ -TrCP and Jade-1 may ensure optimal Wnt pathway regulation. Furthermore, pVHL downregulates  $\beta$ -catenin in a Jade-1-dependent manner and inhibits Wnt signalling, supporting a role for Jade-1 and Wnt signalling in renal tumorigenesis. The pVHL tumour suppressor and the Wnt tumorigenesis pathway are therefore directly linked through Jade-1.**

To identify molecular mediators of Jade-1 activity, we screened a human kidney complementary DNA library with a yeast two-hybrid approach using a transcriptionally inactive truncation of Jade-1 lacking both plant homeodomains (PHDs) (Jade-1 dd) as bait (Supplementary Information, Fig. S1a). Nine strong interactors were found, including  $\beta$ -catenin, an oncoprotein and the key transcriptional co-activator of canonical Wnt signalling<sup>7</sup>.

The Jade-1- $\beta$ -catenin interaction was confirmed in mammalian cells by co-immunoprecipitation (Fig. 1a). The localization and fate of  $\beta$ -catenin depend on Wnt status<sup>7</sup>. Constitutively, in Wnt-off phase,  $\beta$ -catenin is phosphorylated by glycogen synthase kinase (GSK)-3 $\beta$ , binds to the destruction complex in the cytosol and is degraded. In Wnt-on phase, GSK-3 $\beta$  is inhibited;  $\beta$ -catenin dissociates from the destruction

complex and translocates to the nucleus. We therefore examined the binding of endogenous Jade-1 and  $\beta$ -catenin during the different states of Wnt signalling. Wnt signalling was activated by using Wnt-3a ligand or lithium chloride (an inhibitor of GSK-3 $\beta$  that mimics Wnt activation) and inhibited by using Wnt-3a plus dickkopf 1 (DKK1), a competitive antagonist of Wnt-3a (Fig. 1b and Supplementary Information, Fig. S1b). Endogenous Jade-1 co-immunoprecipitated with endogenous  $\beta$ -catenin, and vice versa (Fig. 1b). However, the Jade-1- $\beta$ -catenin interaction was increased in vehicle-treated and Wnt-3a-DKK1-treated cells (Wnt-off phase) in comparison with Wnt-3a-treated cells (Wnt-on phase). Co-localization and profile plots were performed to demonstrate the distribution and abundance of the proteins (Fig. 1c). In Wnt-off phase (Fig. 1c, vehicle-treated),  $\beta$ -catenin was predominantly in the cytosol and cell membrane. Jade-1 was in the cytosol and nucleus, excluding nucleoli<sup>3,8</sup>. Jade-1 and  $\beta$ -catenin were co-localized in the cytosol. Treatment with Wnt-3a resulted in nuclear translocation of  $\beta$ -catenin. However, Jade-1 and  $\beta$ -catenin had different sub-compartmental localizations in the nucleus (Fig. 1c, Wnt-3a-treated), resulting in a decrease in co-localization. Thus, endogenous Jade-1 and endogenous  $\beta$ -catenin interact, and the interaction is greater in Wnt-off phase than in Wnt-on phase.

Jade-1 interacted specifically with the amino terminus of  $\beta$ -catenin (Fig. 1d). Jade-1 showed decreased binding to a naturally occurring, cancer-causing, constitutively active (CA) S33A mutant of  $\beta$ -catenin lacking this GSK-3 $\beta$  phosphorylation site (Fig. 1d). These findings were confirmed by immunofluorescence microscopy of cells expressing Flag-tagged Jade-1 and a Myc-tagged  $\beta$ -catenin series (Supplementary Information, Fig. S1c–e). In Wnt-off phase, Jade-1 co-localized extensively with wild-type  $\beta$ -catenin and the carboxy-terminally truncated  $\beta$ -catenin predominantly in the cytosol, but not with  $\beta$ -catenin S33A or the N-terminally truncated  $\beta$ -catenin (Supplementary Information, Fig. S1d). In contrast, in Wnt-on phase, wild-type  $\beta$ -catenin localized to the nucleus, thereby decreasing co-localization with Jade-1 (Supplementary Information, compare Fig. S1d with Fig. S1e), which is consistent with the reduction in endogenous Jade-1- $\beta$ -catenin binding with Wnt activation. These data indicate that  $\beta$ -catenin

<sup>1</sup>Renal Section, <sup>2</sup>Vascular Biology Unit, <sup>3</sup>Molecular Stress Response Unit, <sup>4</sup>Hematology–Oncology Section, Department of Medicine, Boston University School of Medicine, Boston, Massachusetts 02118, USA. <sup>5</sup>Renal Division, Beth Israel Deaconess Medical Center, Harvard Medical School, Boston, Massachusetts 02118, USA. Correspondence should be sent to H.T.C. (e-mail: htcohen@bu.edu)

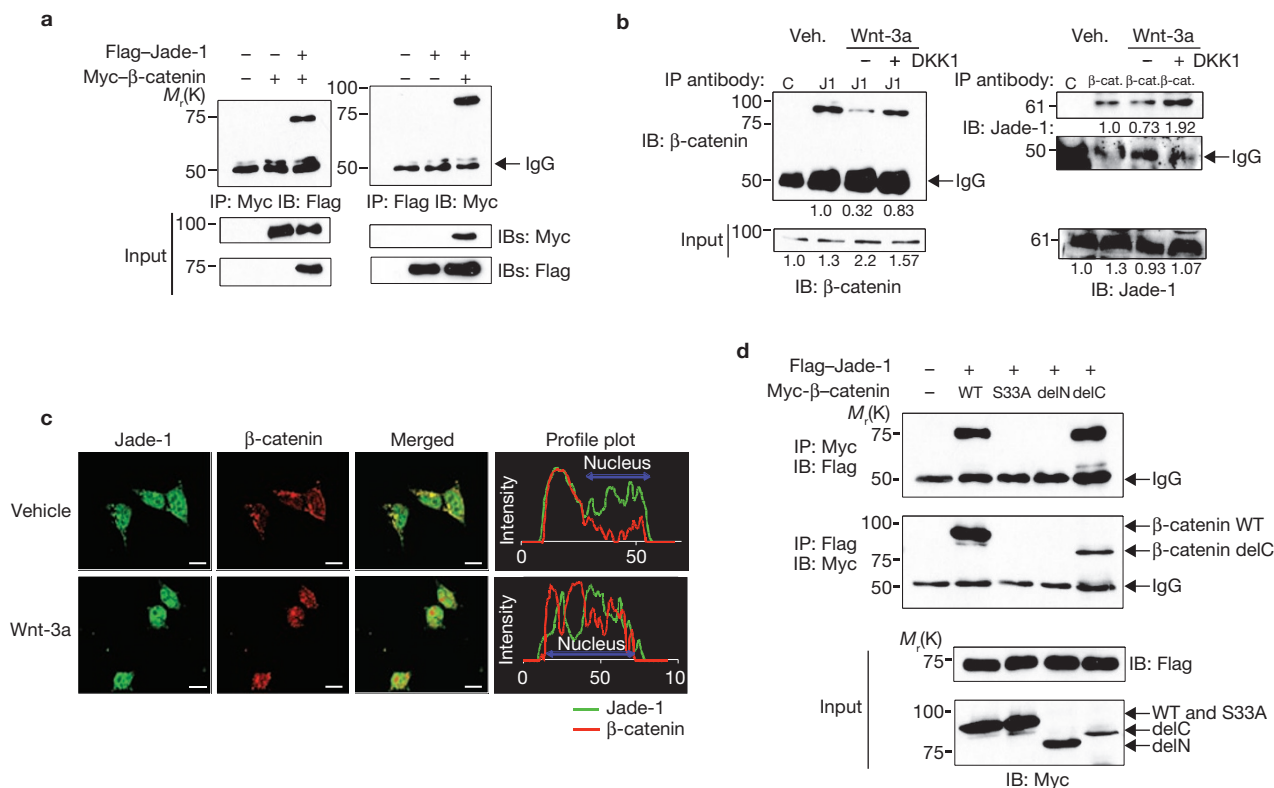


**Figure 1** Jade-1 and  $\beta$ -catenin interact. **(a)** *In vivo* interaction of Jade-1 and  $\beta$ -catenin. Extracts (600  $\mu$ g of protein) from transiently transfected 293T cells were immunoprecipitated (IP) with 1  $\mu$ g of monoclonal Myc-tag or Flag-tag antibodies. Co-immunoprecipitated  $\beta$ -catenin or Jade-1 was detected by immunoblotting (IB). Whole cell lysates (10%) were probed for input. Representative immunoblot of four experiments. **(b)** The interaction of endogenous Jade-1 and endogenous  $\beta$ -catenin is increased in Wnt-off phase. IPs were performed with whole cell lysates of 293T cells pretreated with vehicle (PBS + 0.1% BSA) or 50 ng of Wnt-3a ligand with or without 50 ng of DKK1, using 1  $\mu$ g of either polyclonal anti-Jade-1 antibody (J1) or preimmune serum (C).  $\beta$ -Catenin was immunoprecipitated with monoclonal anti- $\beta$ -catenin antibody ( $\beta$ -cat.) or isotype control (C). Jade-1 was detected with Jade-1 antiserum. Whole cell lysates (10%) were probed for input. The amounts of Jade-1 and  $\beta$ -catenin immunoprecipitated were normalized with IgG. Representative immunoblot of three experiments. Numbers at the left of gels are relative molecular weights. **(c)** Co-localization of endogenous

Jade-1 and endogenous  $\beta$ -catenin is increased in Wnt-off phase. The 293T cells pretreated with vehicle or Wnt-3a (200 ng) for 4 h were fixed and incubated with monoclonal anti- $\beta$ -catenin and polyclonal anti-Jade-1 antibodies. Profile plots were generated with NIH ImageJ to demonstrate quantitative Jade-1 and  $\beta$ -catenin protein distribution. The profile plot represents the signal intensity of each fluorophore along a single line across the midpoint of a representative cell. The x axis is the distance in pixels through the length of a single cell, and the intensity of each fluorophore is plotted on the y axis. Representative image from four experiments. Scale bar, 10  $\mu$ m. **(d)** Identification of the domain of  $\beta$ -catenin required for Jade-1 binding. Extracts from transiently transfected 293T cells were immunoprecipitated. Whole cell lysates (10%) were probed for input.  $\beta$ -Catenin delC and delN constructs lack the C terminus and N terminus of the protein, respectively (Supplementary Fig. S1a). Representative immunoblot of three experiments. Full scans of immunoblots are shown in Supplementary Information, Fig. S7.

N-terminal serine residue 33, or its phosphorylation, is important for optimal binding to Jade-1. We examined the binding of purified recombinant glutathione S-transferase (GST)-tagged Jade-1 and GST-tagged  $\beta$ -catenin in *in vitro* GST pull-down assays. GST-tagged Jade-1 associated with GST-tagged  $\beta$ -catenin (Supplementary Information, Fig. S1f). However, this binding was substantially increased after *in vitro* phosphorylation of  $\beta$ -catenin by the kinases casein kinase 1 and GSK-3 $\beta$  (Supplementary Information, Fig. S1f). GST-tagged Jade-1 did not bind to the N-terminally deleted  $\beta$ -catenin. Overall, Jade-1 directly binds the N terminus of  $\beta$ -catenin, and the interaction is enhanced with  $\beta$ -catenin phosphorylation in Wnt-off phase.

In Wnt-off phase,  $\beta$ -catenin is degraded in a process that depends on the  $\beta$ -catenin N terminus or 'degron'<sup>7,9</sup>. Jade-1 interacts with the N terminus of  $\beta$ -catenin and, in particular, residue S33 (Supplementary Information, Fig. S1a). We therefore examined whether Jade-1 regulates the abundance of  $\beta$ -catenin. Jade-1 downregulated wild-type  $\beta$ -catenin and a C-terminally deleted  $\beta$ -catenin (Fig. 2a). However, Jade-1 had little

effect on an N-terminally deleted  $\beta$ -catenin or  $\beta$ -catenin S33A, which is consistent with the binding pattern of Jade-1 with  $\beta$ -catenin (Fig. 1d).

Endogenous  $\beta$ -catenin exists in three distinct cellular pools<sup>7</sup>. The quantity of endogenous  $\beta$ -catenin protein in the cytosolic and nuclear fractions in three different *Jade-1*-silenced cell lines was at least double that in empty-vector lines (Fig. 2b and Supplementary Information, Fig. S2b–d). The membrane pool of  $\beta$ -catenin was unchanged. Conversely, the amount of  $\beta$ -catenin in the cytosolic and nuclear fractions was substantially lower in *Jade-1*-expressing stable cell lines than in the empty-vector cell lines (Fig. 2c). We then examined the half-life of cytosolic  $\beta$ -catenin. A digitonin-extracted fraction<sup>10</sup> was enriched for cytosol, as demonstrated by the increase in cytosolic markers, but had no membrane contamination (Supplementary Information, Fig. S2e). The half-life of the digitonin-extracted cytosolic  $\beta$ -catenin was increased from 10 min to 90 min in *Jade-1*-silenced 293 cell lines (Fig. 2d). Thus, *Jade-1* silencing substantially stabilized cytosolic  $\beta$ -catenin. The half-life of  $\beta$ -catenin was decreased in the *Jade-1*-expressing renal cancer cell

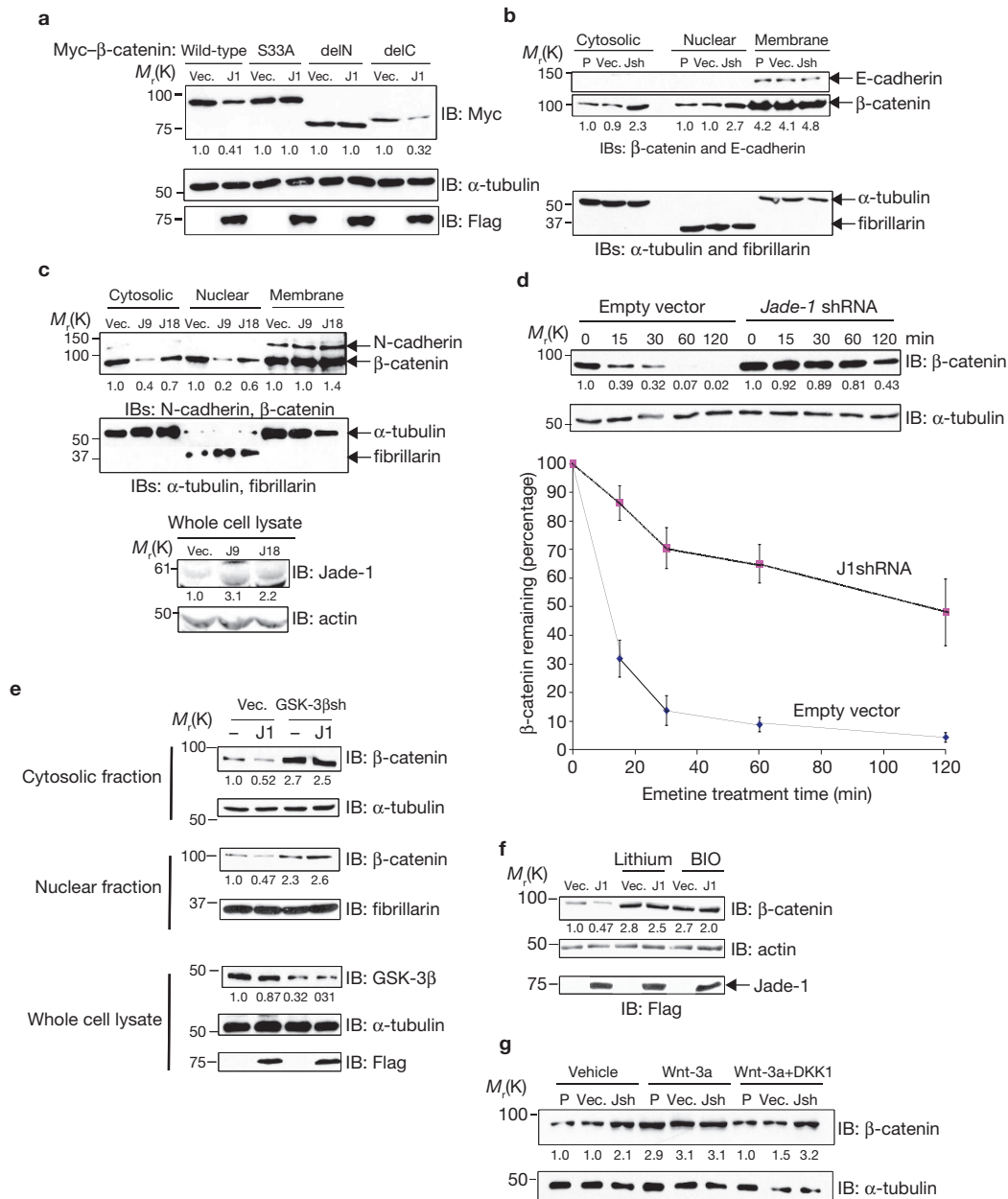


**Figure 2** Jade-1 reduces β-catenin protein abundance. **(a)** Differential regulation of β-catenin constructs by Jade-1. Whole cell lysates of 293T cells transiently transfected with Myc-tagged β-catenin and Flag-tagged Jade-1 (J1) constructs were probed. Diagrams of β-catenin constructs are shown in Supplementary Information, Fig. S1a. Representative immunoblot of five experiments. **(b)** Jade-1 regulates the cytosolic and nuclear fractions but not the membrane fraction of endogenous β-catenin. Cell fractions were prepared from 293 uninfected parental cells (P) or cells infected with empty vector (Vec) or *Jade-1* shRNA lentivirus (Jsh). α-Tubulin, fibrillarin and E-cadherin served as loading controls and cell fraction markers. One of two similar experiments is shown. **(c)** Jade-1 reduces cytosolic and nuclear pools of endogenous β-catenin. Extracts of clonal 786-O renal cancer cell lines stably expressing empty vector (Vec) or Jade-1 (J9 and J18; ref. 5) were probed for β-catenin. Representative immunoblot of three experiments. **(d)** *Jade-1* silencing prolongs the half-life of endogenous cytosolic β-catenin. Digitonin<sup>10</sup> was used to extract cytosolic β-catenin. Upper panels: digitonin extracts of 293 cells infected with empty vector or JshRNA lentiviral

vector and pretreated with 20 μM emetine were probed. Bottom panel: the percentage of β-catenin remaining in the digitonin-extracted fraction was analysed by densitometry after normalization to α-tubulin. The graph shows the mean result of four experiments. Error bars indicate s.e.m. **(e)** *GSK-3β* silencing mitigates regulation of endogenous β-catenin by Jade-1. Transiently transfected 293T cells were sorted by fluorescence-activated cell sorting and replated for 48 h. One of two similar experiments. **(f)** Chemical inhibition of *GSK-3β* mitigates regulation of endogenous β-catenin by Jade-1. Transiently transfected 293T cells were serum-starved for 12–16 h and treated with lithium chloride (10 mM) or 6-bromoindirubin-3'-oxime (BIO, 100 nM) for a further 12 h. Representative immunoblot of four experiments. **(g)** Regulation of endogenous β-catenin by Jade-1 in Wnt-on and Wnt-off phases. The cytosolic fractions of HeLa parental cells (P) or cells infected with empty vector (Vec) or *Jade-1* shRNA (Jsh) lentivirus were treated for 4 h with Wnt-3a (100 ng) with or without DKK1 (100 ng) and probed for β-catenin. Representative immunoblot of four experiments. Full scans of immunoblots are shown in Supplementary Information, Fig. S7.

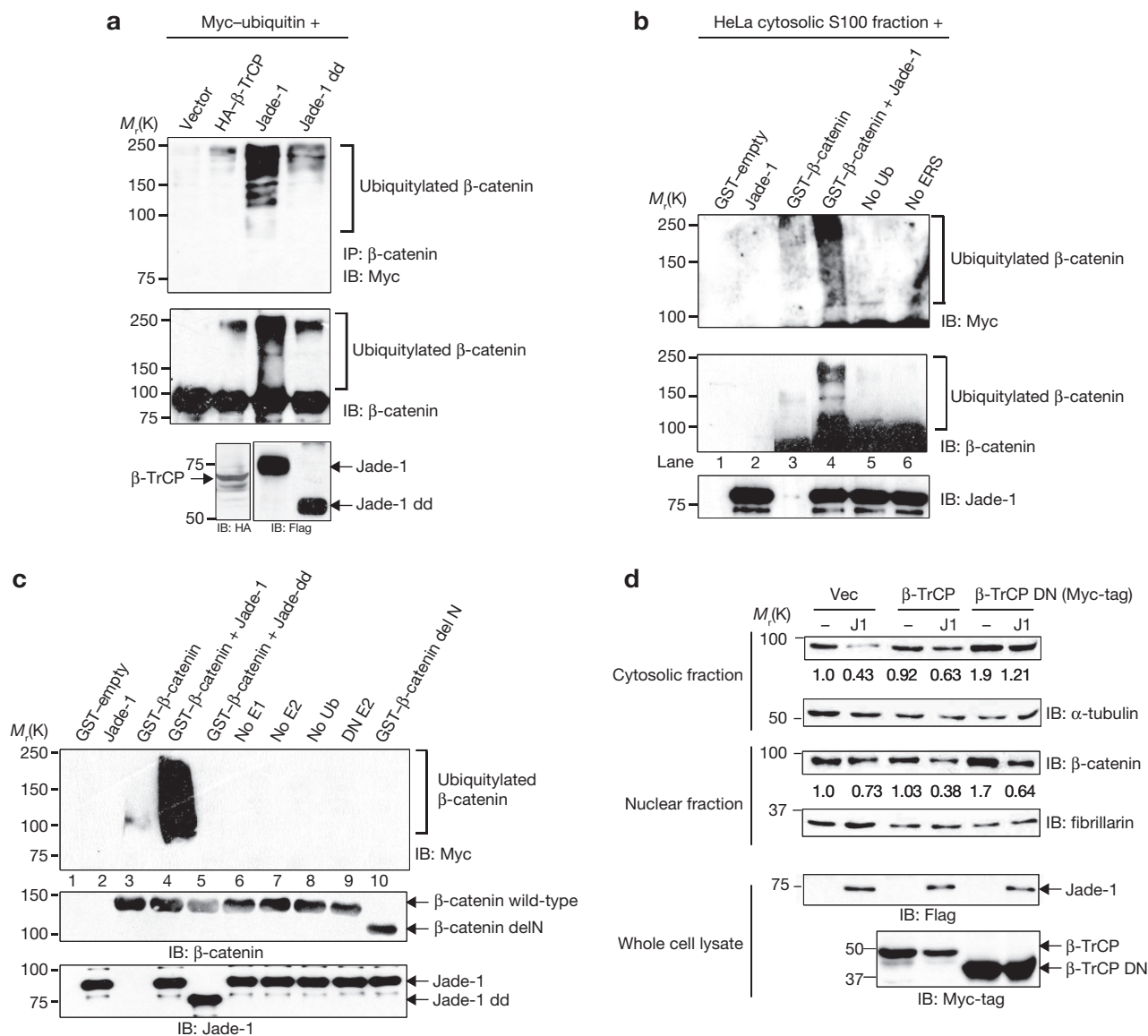


**Figure 3** Jade-1 ubiquitylates  $\beta$ -catenin. **(a)** Deletion of the Jade-1 PHDs substantially decreases endogenous  $\beta$ -catenin ubiquitylation. Whole cell lysates of 293T cells pretreated with MG132 (10  $\mu$ M for 1 h) were immunoprecipitated. The eluate was divided into two equal parts and immunoblotted separately with monoclonal anti-Myc-tag antibody or anti- $\beta$ -catenin antibody. One of two similar experiments. **(b)** *Ex vivo* ubiquitylation of purified  $\beta$ -catenin with the HeLa cell cytosolic S100 fraction. Purified recombinant GST- $\beta$ -catenin on glutathione-Sepharose beads was incubated with HeLa cell S100 fraction, Myc-tagged human recombinant ubiquitin (Ub), recombinant Jade-1 and energy regeneration solution (ERS).  $\beta$ -Catenin eluted from the beads was divided into two equal parts and immunoblotted separately with monoclonal anti-Myc-tag or anti- $\beta$ -catenin antibodies. Lanes designated 'no Ub' or 'no ERS' were reactions lacking only Ub or ERS, respectively. Lane 3 was rearranged from the same blot. One of two similar experiments. **(c)** Jade-1 ubiquitylation of  $\beta$ -catenin *in vitro*, and mapping of the E3 ubiquitin ligase domain on Jade-1. A panel of E2 ubiquitin transferases, including UbcH2, UbcH3, UbcH5a, UbcH5b, UbcH5c,

UbcH6, UbcH7 and UbcHc10, was screened for Jade-1-mediated  $\beta$ -catenin ubiquitylation (data not shown). Jade-1 ubiquitylated  $\beta$ -catenin only in the presence of UbcH6 or UbcH2 (data not shown). Ubiquitylation reactions were reconstituted with GST- $\beta$ -catenin (wild-type or delN) with E1, E2 and E3 ligase, 750 nM Jade-1 (full-length or dd), Myc-tagged recombinant human Ub and MgCl<sub>2</sub>-ATP. Lanes designated 'no E1', 'no E2' and 'no Ub' were reactions with all constituents except E1, E2 or Ub only, respectively. Dominant-negative UbcH6 (DN E2) was used instead of wild-type UbcH6, as a control. GST- $\beta$ -catenin and GST-Jade-1 beads equivalent to that used in the reactions were probed separately with polyclonal anti- $\beta$ -catenin C-terminal antibody or polyclonal anti-Jade-1 antibody. Representative immunoblot of three experiments. **(d)** Jade-1-mediated degradation of endogenous  $\beta$ -catenin is independent of  $\beta$ -TrCP. Whole cell lysates of 293T cells transfected with wild-type or DN  $\beta$ -TrCP, with or without Flag-tagged Jade-1, were probed with anti- $\beta$ -catenin antibody. Representative immunoblot of four experiments. Full scans of immunoblots are shown in Supplementary Information, Fig. S7.

lines (Supplementary Information, Fig. S2f). Thus, Jade-1 regulates the stability of the Wnt-responsive pool of  $\beta$ -catenin.

The degradation of  $\beta$ -catenin depends on GSK-3 $\beta$ . In Wnt-off phase,  $\beta$ -catenin undergoes sequential phosphorylation at residues T41, S37 and

S33 by GSK-3 $\beta$ . Preferential binding of Jade-1 to phospho- $\beta$ -catenin and the lack of binding to  $\beta$ -catenin S33A suggest a possible role for GSK-3 $\beta$  in the regulation of  $\beta$ -catenin by Jade-1 (Fig. 1d and Supplementary Information, Fig. S1f). Moreover, full-length Jade-1 decreased the total

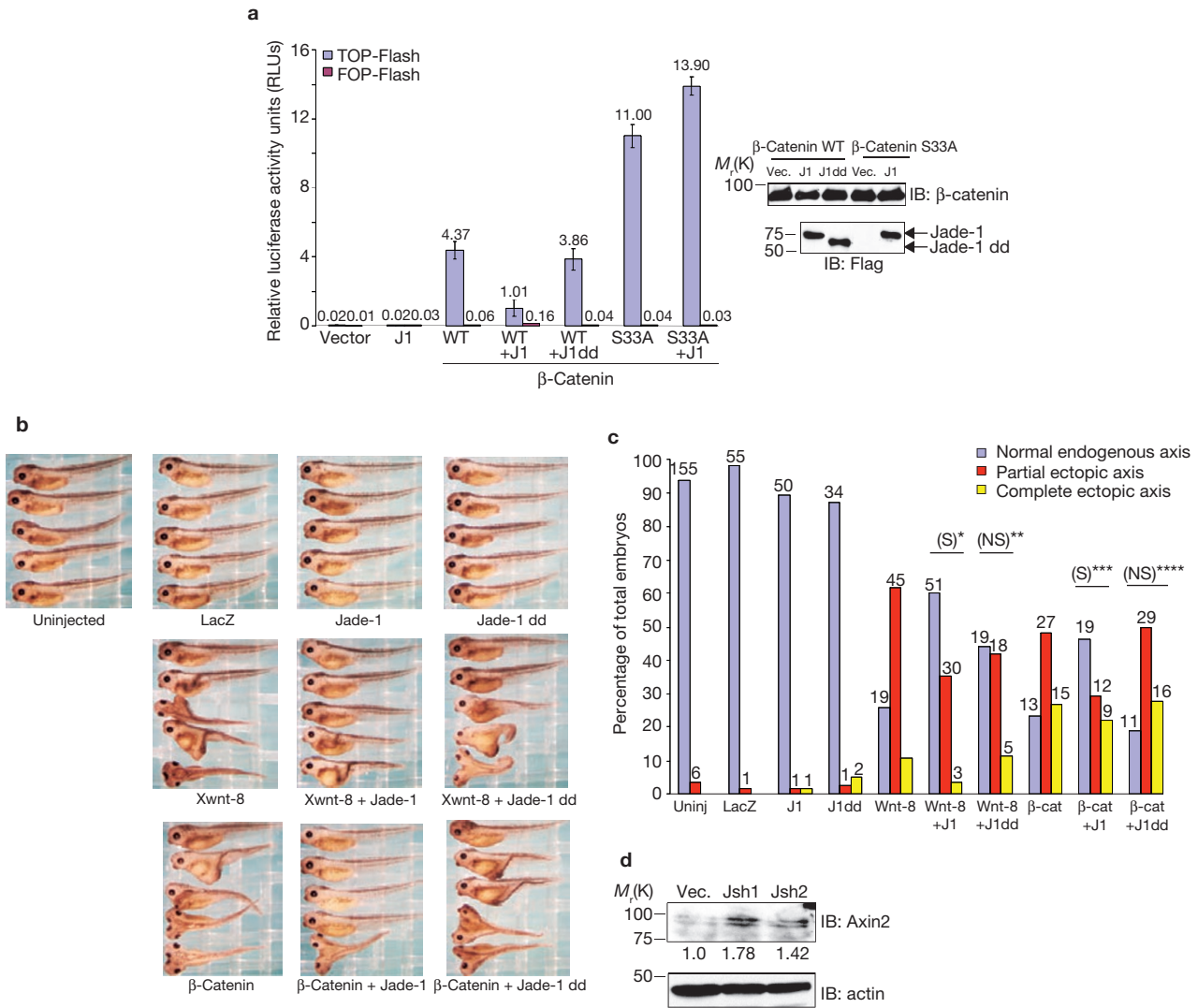


**Figure 4** Jade-1 inhibits canonical Wnt signalling. **(a)** Jade-1 suppresses TCF/β-catenin reporter activity. TCF-responsive promoter–reporter TOP-Flash and non-responsive control reporter FOP-Flash were used. Activity of the Wnt signalling pathway was quantified by measuring relative firefly luciferase activity units (RLUs) normalized to *Renilla* luciferase. The 293T cells were transfected with wild-type β-catenin (WT) or β-catenin S33A and Jade-1 (J1) full-length or Jade-1 dd (J1dd). Mean results of three experiments. Error bars indicate s.e.m. Protein extracts were probed using monoclonal anti-Flag and anti-β-catenin antibodies to examine the expression of constructs. **(b)** Jade-1 inhibits *Xwnt8*-induced and β-catenin-induced ectopic axis formation in *Xenopus laevis* embryos. *Xwnt-8* (0.34–0.45 pg) or β-catenin (100–120 pg) mRNA, with or without *Jade-1* (full-length 0.8 ng or dd 1.2 ng) mRNA, was injected into ventral blastomeres. *LacZ* (1.5 ng) served as a negative control. A total of seven experiments were performed to compare embryos

injected with full-length *Jade-1* and with *Jade-1* dd. **(c)** *Xwnt-8*-induced and β-catenin-induced ectopic axis is inhibited by *Jade-1* in *Xenopus laevis* embryos. The histogram depicts *Xenopus laevis* embryo phenotypes. Numbers at the top of each bar indicate the number of embryos in each category. A  $\chi^2$  test was applied to determine statistical significance: asterisk, *Xwnt-8* with *Jade-1* versus *Xwnt-8* ( $P < 0.0001$ ); two asterisks, *Xwnt-8* with *Jade-1* dd versus *Xwnt-8* ( $P = 0.096$ ); three asterisks, β-catenin with *Jade-1* versus β-catenin ( $P < 0.046$ ); four asterisks, β-catenin with *Jade-1* dd versus β-catenin ( $P = 0.087$ ). S, statistically significant; NS, not significant. **(d)** Jade-1 regulates endogenous Wnt targets. Whole cell lysates of 293 cells infected with empty vector (Vec) or *Jade-1*-silencing lentiviral constructs (Jsh1 and Jsh2) were probed for endogenous Axin2 and actin. One of two similar experiments. Full scans of immunoblots are shown in Supplementary Information, Fig. S7.

quantity of β-catenin, predominantly as a result of a decrease in the quantity of phospho-β-catenin (Supplementary Information, Fig. S3a). Thus, Jade-1 preferentially regulates phospho-β-catenin. This observation further suggests that GSK-3β may be particularly important for the regulation of β-catenin by Jade-1. Indeed, the regulation of β-catenin by Jade-1 was mitigated by the silencing or chemical inhibition of GSK-3β (Fig. 2e, f). Similarly, the effect of *Jade-1* silencing on the abundance of β-catenin was decreased in Wnt-on phase, when GSK-3β activity is inhibited (Fig. 2g and Supplementary Information, Fig. S3b). Overall, these

data indicate that Jade-1 requires intact GSK-3β kinase activity for full inhibition of β-catenin.

β-Catenin undergoes proteasomal degradation<sup>11</sup>. Inhibition of proteasome activity with MG132 completely abrogated the effect of Jade-1 on the abundance of β-catenin (Supplementary Information, Fig. S3c). Moreover, in the presence of Jade-1 and proteasomal inhibition, very high-molecular-mass species of β-catenin accumulated (Supplementary Information, Fig. S3d), suggesting that Jade-1 may enhance the ubiquitination and degradation of β-catenin.

Protein ubiquitylation depends on substrate recognition by a highly selective E3 ubiquitin ligase. PHD proteins such as MEK kinase 1 (MEKK1) and modulator of immune recognition (MIR) show E3 ubiquitin ligase activity<sup>12,13</sup>. Jade-1 has two PHDs<sup>3</sup> that align well with the PHDs of MEKK1, MIR1, MIR2 and c-MIR (Supplementary Information, Fig. S4a). We therefore reasoned that Jade-1, through its PHDs, might ubiquitylate  $\beta$ -catenin. Deletion of the PHDs reduced the effect of Jade-1 on  $\beta$ -catenin (Supplementary Information, Fig. S4b). Next, endogenous  $\beta$ -catenin was immunoprecipitated, and its ubiquitylation was examined in the presence of Myc-tagged ubiquitin and Jade-1, Jade-1 dd or  $\beta$ -TrCP<sup>6</sup> (Fig. 3a). Minimal  $\beta$ -catenin ubiquitylation was observed with  $\beta$ -TrCP under these conditions, possibly as a result of lower expression of  $\beta$ -TrCP or the fact that the other components of the  $\beta$ -TrCP Skp/Cullin/F-box protein (SCF) complex were not co-expressed. Robust  $\beta$ -catenin polyubiquitylation was observed with full-length Jade-1, whereas deletion of the PHDs substantially decreased the ubiquitylation of  $\beta$ -catenin (Fig. 3a). Ubiquitylation of  $\beta$ -catenin appeared as a smear, most prominently in the presence of full-length Jade-1. Because 293T cells are in Wnt-off status under basal conditions, these data indicate that Jade-1 promotes the ubiquitylation of endogenous  $\beta$ -catenin in Wnt-off phase.

The ubiquitylation of  $\beta$ -catenin *in vitro* was then examined. GST-purified  $\beta$ -catenin was incubated with the cytosolic S100 fraction of HeLa cells. Ubiquitylation of  $\beta$ -catenin was observed in the presence of Jade-1 (Fig. 3b). To address the question of whether Jade-1 directly ubiquitylates  $\beta$ -catenin and to map the E3 ubiquitin ligase domain within Jade-1, we reconstituted ubiquitylation reactions with all purified components (Fig. 3c and Supplementary Fig. S4c). Ubiquitylation of  $\beta$ -catenin was observed with Jade-1 in a dose-dependent manner (Supplementary Information, Fig. S4c, lanes 4–6). Deletion of the Jade-1 PHDs or the  $\beta$ -catenin N terminus abrogated the ubiquitylation of  $\beta$ -catenin (Fig. 3c, lanes 5 and 10, and Supplementary Information, Fig. S4c, lanes 7 and 12). Thus, purified Jade-1 ubiquitylates non-phosphorylated GST-tagged  $\beta$ -catenin, and the Jade-1 PHDs are necessary for E3 ubiquitin ligase activity.

To examine the relationship between Jade-1-mediated and  $\beta$ -TrCP-mediated  $\beta$ -catenin degradation, dominant-negative (DN)  $\beta$ -TrCP lacking the F box was used to antagonize both  $\beta$ -TrCP1 and  $\beta$ -TrCP2 (ref. 14). DN  $\beta$ -TrCP doubled the expression of endogenous  $\beta$ -catenin (Fig. 3d). Jade-1 was still able to downregulate  $\beta$ -catenin in the presence of DN  $\beta$ -TrCP (Fig. 3d), which suggests that Jade-1 regulates  $\beta$ -catenin independently of  $\beta$ -TrCP.

The biological significance of the Jade-1– $\beta$ -catenin interaction was evaluated in T-cell factor (TCF)/ $\beta$ -catenin transcription assays. Full-length Jade-1, but not Jade-1 dd, inhibited a TOP-Flash promoter-reporter 4.3-fold (Fig. 4a). Jade-1 had no effect on the transcriptional activity of  $\beta$ -catenin S33A (Fig. 4a). These observations are consistent with the effect of Jade-1 on protein levels of wild-type  $\beta$ -catenin and  $\beta$ -catenin S33A (Fig. 2a). Intriguingly, significant inducible endogenous Wnt activity was observed in *Jade-1*-silenced cell lines (Supplementary Information, Fig. S5a), which is consistent with the stabilization of endogenous  $\beta$ -catenin in these lines.

Because Jade-1 destabilizes  $\beta$ -catenin and inhibits  $\beta$ -catenin-mediated transactivation, we reasoned that Jade-1 might inhibit the canonical Wnt pathway *in vivo*. We used a functional assay for canonical Wnt signalling, namely the formation of an ectopic axis in *Xenopus laevis* embryos by ventral injection of *Xwnt-8* or  $\beta$ -catenin messenger RNA<sup>15</sup>. Full-length *Jade-1*, but not *Jade-1 dd*, significantly inhibited both *Xwnt-8*-induced

and  $\beta$ -catenin-induced ectopic axis formation in developing *Xenopus laevis* embryos (Fig. 4b, c, and Supplementary Information, Fig. S5b). These data suggest that Jade-1 has the capacity to suppress Wnt activity during Wnt-on phase *in vivo*. This is plausible in view of the appreciable interaction of Jade-1 and  $\beta$ -catenin in Wnt-on phase (Figs. 1b and Supplementary Information Fig. S1b) and Jade-1 binding and ubiquitylation of non-phosphorylated  $\beta$ -catenin (Fig. 3b, c, and Supplementary Information, Fig. S1f). The specific Wnt target Axin2 (ref. 16) was also increased in *Jade-1*-silenced 293 cell lines (Fig. 4d). Other Wnt targets, such as cyclin D1 and c-Myc, were increased in *Jade-1*-silenced cell lines (Supplementary Information, Fig. S5c). Full-length Jade-1, but not Jade-1 dd, decreased protein levels of c-Myc (Supplementary Information, Fig. S5d). Thus, Jade-1 is an inhibitor of canonical Wnt signalling.

Jade-1 protein is stabilized by wild-type pVHL but not by mutated pVHL associated with renal cancer<sup>3,4</sup>. We proposed that pVHL might regulate  $\beta$ -catenin through Jade-1. First, we compared  $\beta$ -catenin abundance in *VHL*-deficient and *VHL*-intact renal cancer cell lines (Fig. 5a). Endogenous cytosolic and nuclear pools of  $\beta$ -catenin were severalfold lower in *VHL*-intact cell lines than in *VHL*-deficient cell lines (Fig. 5a). This result can be explained by our previous observations that Jade-1 levels are significantly lower in *VHL*-deficient cell lines<sup>5</sup>. Next, the reintroduction of pVHL in 786-O cells increased endogenous Jade-1 (refs 4, 5) and substantially decreased endogenous  $\beta$ -catenin levels (Fig. 5b and Supplementary Information, Fig. S6a). Knockdown of *VHL* with short interfering RNA (siRNA) oligonucleotides resulted in downregulation of Jade-1 and the accumulation of  $\beta$ -catenin (Fig. 5c and Supplementary Information, Fig. S6b)<sup>17</sup>.

To examine specifically whether Jade-1 mediates pVHL downregulation of  $\beta$ -catenin, we compared  $\beta$ -catenin regulation by wild-type pVHL and by truncated forms of pVHL that do not stabilize Jade-1 (ref. 4) (Fig. 5d). pVHL del96–122 and naturally occurring, cancer-causing truncations such as pVHL 1–143 and pVHL 1–175, which have little or no effect on Jade-1 stability<sup>4</sup>, had minimal effect on  $\beta$ -catenin (Fig. 5d). We also knocked down *Jade-1* in the presence of pVHL. Endogenous Jade-1 levels were increased by pVHL, an effect blocked by *Jade-1* knockdown (Supplementary Information, Fig. S6c). Downregulation of  $\beta$ -catenin by pVHL was substantially mitigated by *Jade-1* knockdown (Supplementary Information, Fig. S6c). Furthermore, wild-type pVHL, but not pVHL del96–122, suppressed the transcriptional activity of  $\beta$ -catenin (Supplementary Information, Fig. S6d). Specific Wnt targets such as LEF1 (ref. 18) and cyclin D1 were decreased in pVHL-expressing renal cancer cell lines (Fig. 5e). Wild-type pVHL, but not pVHL del96–122, also decreased Axin2 in 293T cells (Supplementary Information, Fig. S6e). Overall, these data indicate that pVHL inhibits  $\beta$ -catenin and canonical Wnt signalling and that Jade-1 is a critical mediator of these effects.

To determine whether pVHL is able to reduce endogenous Wnt signalling *in vivo*, and to examine the difference in the suppression of Wnt activity by wild-type pVHL and pVHL del96–122, we injected wild-type *VHL* or *VHL del96–122* mRNA into the dorsal blastomeres of *Xenopus laevis* embryos, in which canonical Wnt signalling is necessary for dorsal development<sup>19</sup>. Inhibition of dorsal axis formation in *Xenopus laevis* embryos is demonstrated by a reduction of dorsoanterior structures (small eyes, microcephaly or anencephaly) measured with a dorsoanterior index (DAI) scale<sup>19</sup>. Wild-type pVHL suppressed formation of the dorsal axis significantly more than pVHL del96–122 when expressed at

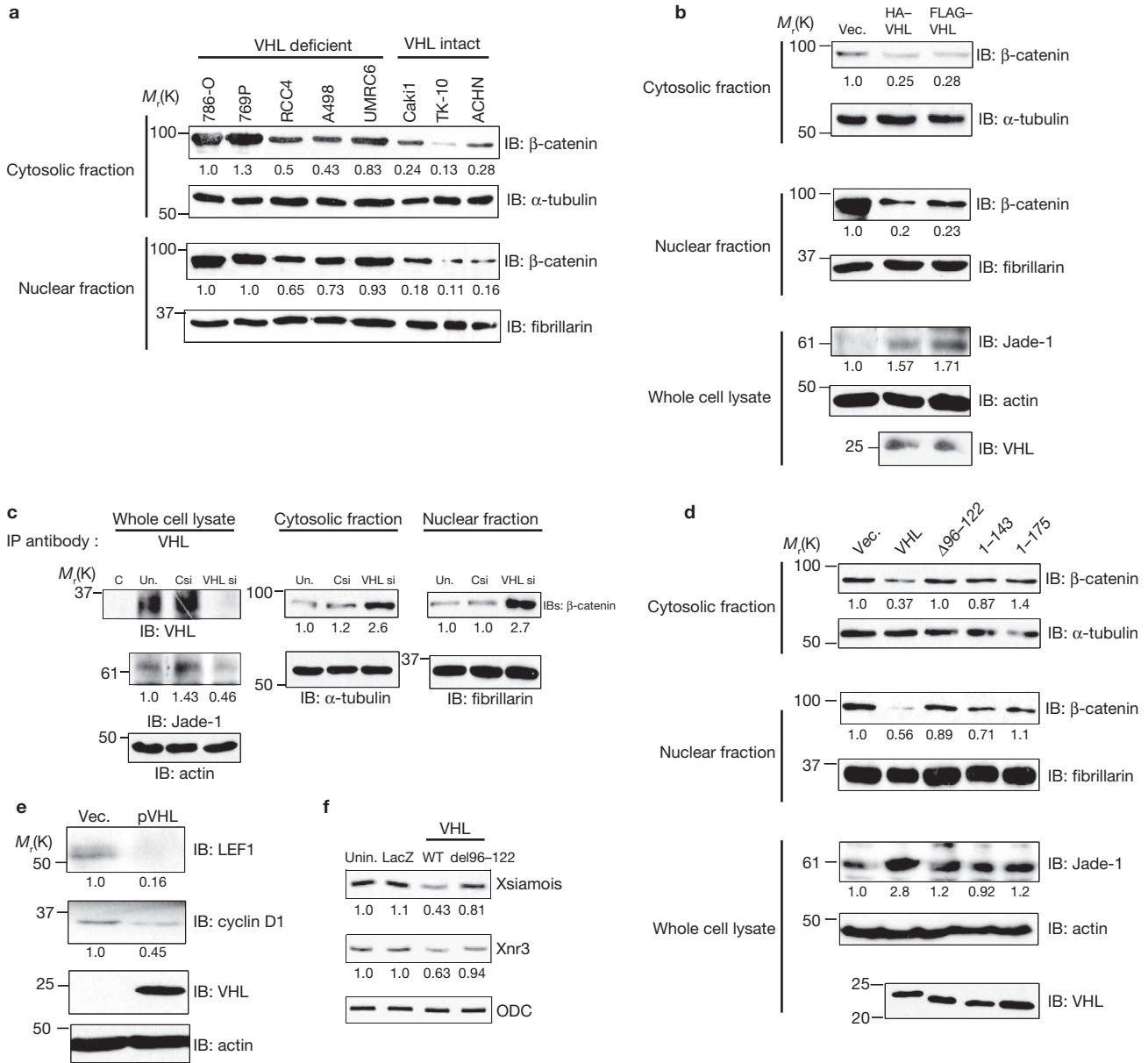


**Figure 5** pVHL regulates endogenous β-catenin through Jade-1. **(a)** β-Catenin protein levels depend on *VHL* status in renal cancer cell lines. Cytosolic and nuclear fractions of renal-cell carcinoma cell lines were probed for endogenous β-catenin protein. One of two similar experiments. **(b)** pVHL downregulates endogenous β-catenin. Extracts from 786-O cells stably expressing empty vector (Vec.) or pVHL were probed for endogenous β-catenin protein. Jade-1 and pVHL expression was detected with polyclonal anti-Jade-1 and monoclonal anti-pVHL antibodies. Representative immunoblot of three experiments. **(c)** *VHL* knockdown increases the abundance of endogenous β-catenin. To confirm *VHL* knockdown, pVHL was immunoprecipitated with polyclonal anti-pVHL or control (C) antibody from untransfected (Un.) 293T cells or 293T cells transfected with *VHL* (VHLsi) or control siRNA (Csi) oligonucleotides because endogenous pVHL abundance is low<sup>17</sup>. Cell fractions were probed for endogenous Jade-1 and endogenous β-catenin protein. Representative immunoblot of three experiments. **(d)** Differential regulation of endogenous β-catenin

by wild-type pVHL and pVHL truncations that do not stabilize Jade-1. Extracts of 293T cells transfected with wild-type pVHL, pVHL del96–122 (Δ96–122), pVHL 1–143 and pVHL 1–175 were probed for pVHL, endogenous β-catenin and endogenous Jade-1 by immunoblotting. One of two similar experiments. **(e)** pVHL suppresses endogenous Wnt targets. Whole cell lysates of empty vector (Vec.) or pVHL-expressing 786-O cell lines were probed for pVHL and endogenous LEF1 and cyclin D1. Representative immunoblot of three experiments. **(f)** Wild-type pVHL, but not pVHL del96–122, suppresses β-catenin/TCF target genes. *In vitro* transcribed, capped *LacZ* (0.288 ng), wild-type *VHL* (WT) (0.194 ng) or *VHL del96–122* (0.293 ng) mRNA was injected into dorsal blastomeres of *Xenopus laevis* embryos. Injected embryos were harvested at stage 10 for RT-PCR. Semiquantitative RT-PCR analysis of the Wnt targets *Xsiamois* and *Xnr3* was performed in whole embryos. *ODC* served as control. Unin., uninjected. Full scans of immunoblots and RT-PCR analyses are shown in Supplementary Information, Fig. S7.

the same level (Supplementary Information, Fig. S6f, g). As expected, inhibition of endogenous axis by wild-type pVHL was associated with greater suppression of β-catenin/TCF target genes *Xsiamois* and *Xnr3*

than by pVHL del96–122 (Fig. 5f). Thus, pVHL inhibits canonical Wnt signalling *in vivo*, and pVHL del96–122, which binds and regulates Jade-1 only minimally<sup>4,5</sup>, had little effect on dorsal axis formation and Wnt target

genes in *Xenopus laevis* embryos. These data further support the role of Jade-1 as a critical mediator of the regulation of  $\beta$ -catenin by pVHL.

In this study we have shown that Jade-1 is an E3 ubiquitin ligase for  $\beta$ -catenin and that the Jade-1 PHDs are essential for this function. Moreover, Jade-1 is a critical mediator of the inhibition of  $\beta$ -catenin and canonical Wnt signalling by pVHL. Jade-1 is anti-proliferative and pro-apoptotic, whereas  $\beta$ -catenin is pro-proliferative, anti-apoptotic and oncogenic<sup>7</sup>. The tumour suppressor activity of Jade-1 may therefore be due in part to inhibition of  $\beta$ -catenin.

Several ubiquitin ligases for  $\beta$ -catenin have now been identified<sup>9,20,21</sup>, but only  $\beta$ -TrCP and Jade-1 show Wnt responsiveness, suggesting that they are both important in the physiology and pathophysiology of canonical Wnt signalling. Endogenous  $\beta$ -TrCP resides in the cytosol and is capable of binding and ubiquitylating phosphorylated  $\beta$ -catenin<sup>6,9,22,23</sup>. In contrast, endogenous Jade-1 resides in the cytosol but is found primarily in the nucleus<sup>3,8</sup> and is capable of binding and ubiquitylating both phosphorylated and non-phosphorylated  $\beta$ -catenin. Thus, Jade-1 and  $\beta$ -TrCP have only partly overlapping subcellular locations and have differing specificities for the forms of  $\beta$ -catenin. These differences may explain why *Jade-1* silencing cannot be completely compensated for by  $\beta$ -TrCP (Fig. 2b, d, and Supplementary Information, Fig. S2b–d). Moreover, Jade-1 seems to act more distally in the canonical Wnt cascade, affecting  $\beta$ -catenin in the nucleus. This may make Jade-1 responsible for the fine control of  $\beta$ -catenin levels.

Jade-1 functions as a single-subunit E3 ubiquitin ligase for  $\beta$ -catenin, whereas  $\beta$ -TrCP requires the formation of a multi-subunit protein complex. The PHD functions as an adaptor-type E3 ubiquitin ligase, directly transferring the ubiquitin moiety to the substrate<sup>13</sup>. Control of Jade-1 may therefore be a simpler and perhaps more efficient way of regulating  $\beta$ -catenin abundance. It is likely that the cell exploits the distinct functional and contextual differences between  $\beta$ -TrCP and Jade-1 to ensure effective regulation of Wnt signalling.

$\beta$ -catenin is emerging as a key molecule in the pathogenesis of renal cancer and renal cystic disease. For example, increased  $\beta$ -catenin activity in renal epithelium in mice results in the robust formation of renal cysts and tumours<sup>24–26</sup>. In renal cancer, methylation of the *APC* gene promoter is common<sup>27</sup>. pVHL was recently shown to inhibit the HGF-mediated tyrosine phosphorylation of  $\beta$ -catenin<sup>28</sup>. These observations further strengthen the role of Wnt signalling in renal-cell carcinoma. Jade-1 and pVHL may also participate in other forms of cystic kidney disease, for which evidence of dysregulated Wnt signalling is increasing<sup>26,29</sup>.

Our data suggest that the inhibition of Wnt signalling by Jade-1 is a new tumour suppressor axis for pVHL. Furthermore, these findings directly link the kidney-specific pVHL tumour suppressor pathway and the Wnt signalling cascade, a more general tumorigenesis pathway. Jade-1 and  $\beta$ -catenin may therefore represent therapeutic targets in renal-cell carcinoma. □

## METHODS

***In vitro* ubiquitylation reaction.** Ubiquitylation reactions were reconstituted in 30  $\mu$ l with ubiquitylation buffer (50 mM Tris-HCl pH 7.5, 0.5 mM dithiothreitol) containing 225 nM E1 activating enzyme (Boston Biochem), 500 nM E2 conjugase, 600  $\mu$ M Myc-tagged ubiquitin (Boston Biochem), 1 mM MgCl<sub>2</sub>-ATP, 750 nM Jade-1 and 2.8  $\mu$ M GST- $\beta$ -catenin on glutathione beads and incubated at 37 °C for 60 min. Reactions without E1, E2 or ubiquitin, or with a DN E2 (mutation of active-site cysteine to serine) served as negative controls.

***Xenopus* embryo injection and phenotype evaluation.** Embryos were fertilized *in vitro*, dejellied in 2% cysteine (pH 7.8) and maintained in 0.1  $\times$  Marc's Modified Ringer's medium (MMR). For microinjection, embryos were transferred to 1.5% Ficoll (Pharmacia) in 0.5  $\times$  MMR and injected at stages 2 or 3. Two blastomeres were injected ventrally with 10 nl of *LacZ* or *Xwnt-8* mRNA with or without *Jade-1* mRNA (full-length or dd), or dorsally with *LacZ* or *VHL* (wild-type or VHL del96–122) mRNA. Embryos were fixed and analysed as described previously<sup>30–32</sup>.

**RT-PCR.** RNA extraction, reverse transcription, PCR, the primer sequence for *Xsiamois*, *Xnr3* and *ODC*, and PCR conditions have been described previously<sup>31</sup>. RNA (2.8  $\mu$ g, measured by Nanodrop; Thermo Fischer Scientific) was used for cDNA preparation.

**Further details.** See Supplementary Methods for details of cell lines, constructs, antibodies, yeast two-hybrid screen, immunoblotting, immunoprecipitation, cellular fractionation, GST purification, *in vivo* ubiquitylation, synthesis of capped RNAs, *Xenopus* injection and phenotype evaluation.

*Note: Supplementary Information is available on the Nature Cell Biology website.*

## ACKNOWLEDGEMENTS

We thank Z.-X. Xiao (Boston University) for insightful suggestions and careful review of the manuscript; K. Symes, M. Malikova and E. Smith (all of Boston University) for *Xenopus laevis* embryos; R. Kemler (Max Planck Institute for Immunobiology, Germany) for providing the  $\beta$ -catenin S33A construct; W. Birchmeier (Max Delbrück Center for Molecular Medicine, Germany) for  $\beta$ -catenin C and N terminus deletion constructs; and R. Benarous (Institute Pasteur, France) for wild-type and DN  $\beta$ -TrCP in pcDNA3.1 Myc/His vector. This work was supported by fellowship grants from the National Kidney Foundation and Polycystic Kidney Disease Foundation (to V.C.C.) and by National Institutes of Health (NIH) Training Grant T32 DK07053 (for V.C.C. and R.L.F.); by American Heart Association grant SDG 0535485T and American Cancer Society grant IRG-72-001-32-IRG (to M.V.P.); by a pilot research grant from the Department of Medicine at Boston University School of Medicine and a Karin Grunebaum Junior Faculty Cancer Research Award (to I.D.); and by NIH grants R01 CA71796 (to D.C.S.) and R01 CA79830 and R01 DK67569 (to H.T.C.). Part of this work was presented at the American Society of Nephrology annual meeting in San Diego, California, USA, in November 2006, and at the American Society of Nephrology annual meeting in San Francisco, California, USA, in November 2007.

## COMPETING FINANCIAL INTERESTS

The authors declare no competing financial interests.

Published online at <http://www.nature.com/naturecellbiology/>  
Reprints and permissions information is available online at <http://npg.nature.com/reprintsandpermissions/>

- Maxwell, P. H. *et al.* The tumour suppressor protein VHL targets hypoxia-inducible factors for oxygen-dependent proteolysis. *Nature* **399**, 271–275 (1999).
- Cohen, H. T. & McGovern, F. J. Renal-cell carcinoma. *N. Engl. J. Med.* **353**, 2477–2490 (2005).
- Zhou, M. I. *et al.* The von Hippel–Lindau tumor suppressor stabilizes novel plant homeodomain protein Jade-1. *J. Biol. Chem.* **277**, 39887–39898 (2002).
- Zhou, M. I., Wang, H., Foy, R. L., Ross, J. J. & Cohen, H. T. Tumor suppressor von Hippel–Lindau (VHL) stabilization of Jade-1 protein occurs through plant homeodomains and is VHL mutation dependent. *Cancer Res.* **64**, 1278–1286 (2004).
- Zhou, M. I. *et al.* Jade-1, a candidate renal tumor suppressor that promotes apoptosis. *Proc. Natl Acad. Sci. USA* **102**, 11035–11040 (2005).
- Winston, J. T. *et al.* The SCF $\beta$ -TRCP-ubiquitin ligase complex associates specifically with phosphorylated destruction motifs in I $\kappa$ B $\alpha$  and stimulates I $\kappa$ B $\alpha$  ubiquitination *in vitro*. *Genes Dev.* **13**, 270–283 (1999).
- Nusse, R. Wnt signaling in disease and in development. *Cell Res.* **15**, 28–32 (2005).
- Panchenko, M. V., Zhou, M. I. & Cohen, H. T. von Hippel–Lindau partner Jade-1 is a transcriptional co-activator associated with histone acetyltransferase activity. *J. Biol. Chem.* **279**, 56032–56041 (2004).
- Latres, E., Chiari, D. S. & Pagano, M. The human F box protein  $\beta$ -Trcp associates with the Cul1/Skp1 complex and regulates the stability of  $\beta$ -catenin. *Oncogene* **18**, 849–854 (1999).
- Schulz, I. Permeabilizing cells: some methods and applications for the study of intracellular processes. *Methods Enzymol.* **192**, 280–300 (1990).
- Aberle, H., Bauer, A., Stappert, J., Kispert, A. & Kemler, R.  $\beta$ -Catenin is a target for the ubiquitin–proteasome pathway. *EMBO J.* **16**, 3797–3804 (1997).
- Coscoy, L., Sanchez, D. J. & Ganem, D. A novel class of herpesvirus-encoded membrane-bound E3 ubiquitin ligases regulates endocytosis of proteins involved in immune recognition. *J. Cell Biol.* **155**, 1265–1273 (2001).
- Lu, Z., Xu, S., Joazeiro, C., Cobb, M. H. & Hunter, T. The PHD domain of MEKK1 acts as an E3 ubiquitin ligase and mediates ubiquitination and degradation of ERK1/2. *Mol. Cell* **9**, 945–956 (2002).



14. Belaidouni, N. *et al.* Overexpression of human  $\beta$  TrCP1 deleted of its F box induces tumorigenesis in transgenic mice. *Oncogene* **24**, 2271–2276 (2005).
15. McCrea, P. D., Brieher, W. M. & Gumbiner, B. M. Induction of a secondary body axis in *Xenopus* by antibodies to  $\beta$ -catenin. *J. Cell Biol.* **123**, 477–484 (1993).
16. Jho, E. H. *et al.* Wnt/ $\beta$ -catenin/Tcf signaling induces the transcription of Axin2, a negative regulator of the signaling pathway. *Mol. Cell. Biol.* **22**, 1172–1183 (2002).
17. Iliopoulos, O., Ohh, M. & Kaelin, W. G. Jr. pVHL19 is a biologically active product of the von Hippel–Lindau gene arising from internal translation initiation. *Proc. Natl Acad. Sci. USA* **95**, 11661–11666 (1998).
18. Hovanes, K. *et al.*  $\beta$ -Catenin-sensitive isoforms of lymphoid enhancer factor-1 are selectively expressed in colon cancer. *Nature Genet.* **28**, 53–57 (2001).
19. Larabell, C. A. *et al.* Establishment of the dorso-ventral axis in *Xenopus* embryos is presaged by early asymmetries in  $\beta$ -catenin that are modulated by the Wnt signaling pathway. *J. Cell Biol.* **136**, 1123–1136 (1997).
20. Liu, J. *et al.* Siah-1 mediates a novel  $\beta$ -catenin degradation pathway linking p53 to the adenomatous polyposis coli protein. *Mol. Cell* **7**, 927–936 (2001).
21. Nastasi, T. *et al.* Ozz-E3, a muscle-specific ubiquitin ligase, regulates  $\beta$ -catenin degradation during myogenesis. *Dev. Cell* **6**, 269–282 (2004).
22. Hart, M. *et al.* The F-box protein  $\beta$ -TrCP associates with phosphorylated  $\beta$ -catenin and regulates its activity in the cell. *Curr. Biol.* **9**, 207–210 (1999).
23. Kitagawa, M. *et al.* An F-box protein, FWD1, mediates ubiquitin-dependent proteolysis of  $\beta$ -catenin. *EMBO J.* **18**, 2401–2410 (1999).
24. Sansom, O. J., Griffiths, D. F., Reed, K. R., Winton, D. J. & Clarke, A. R. Apc deficiency predisposes to renal carcinoma in the mouse. *Oncogene* **24**, 8205–8210 (2005).
25. Qian, C. N. *et al.* Cystic renal neoplasia following conditional inactivation of Apc in mouse renal tubular epithelium. *J. Biol. Chem.* **280**, 3938–3945 (2005).
26. Saadi-Kheddouci, S. *et al.* Early development of polycystic kidney disease in transgenic mice expressing an activated mutant of the  $\beta$ -catenin gene. *Oncogene* **20**, 5972–5981 (2001).
27. Battagli, C. *et al.* Promoter hypermethylation of tumor suppressor genes in urine from kidney cancer patients. *Cancer Res.* **63**, 8695–8699 (2003).
28. Peruzzi, B., Athauda, G. & Bottaro, D. P. The von Hippel–Lindau tumor suppressor gene product represses oncogenic  $\beta$ -catenin signaling in renal carcinoma cells. *Proc. Natl Acad. Sci. USA* **103**, 14531–14536 (2006).
29. Simons, M. *et al.* Inversin, the gene product mutated in nephronophthisis type II, functions as a molecular switch between Wnt signaling pathways. *Nature Genet.* **37**, 537–543 (2005).
30. Nieuwkoop, J. & Faber, J. *Normal Table of Xenopus laevis* (North-Holland, Amsterdam, 1967).
31. Dominguez, I. *et al.* Protein kinase CK2 is required for dorsal axis formation in *Xenopus* embryos. *Dev. Biol.* **274**, 110–124 (2004).
32. Kao, K. R. & Elinson, R. P. The entire mesodermal mantle behaves as Spemann's organizer in dorsoanterior enhanced *Xenopus laevis* embryos. *Dev. Biol.* **127**, 64–77 (1988).

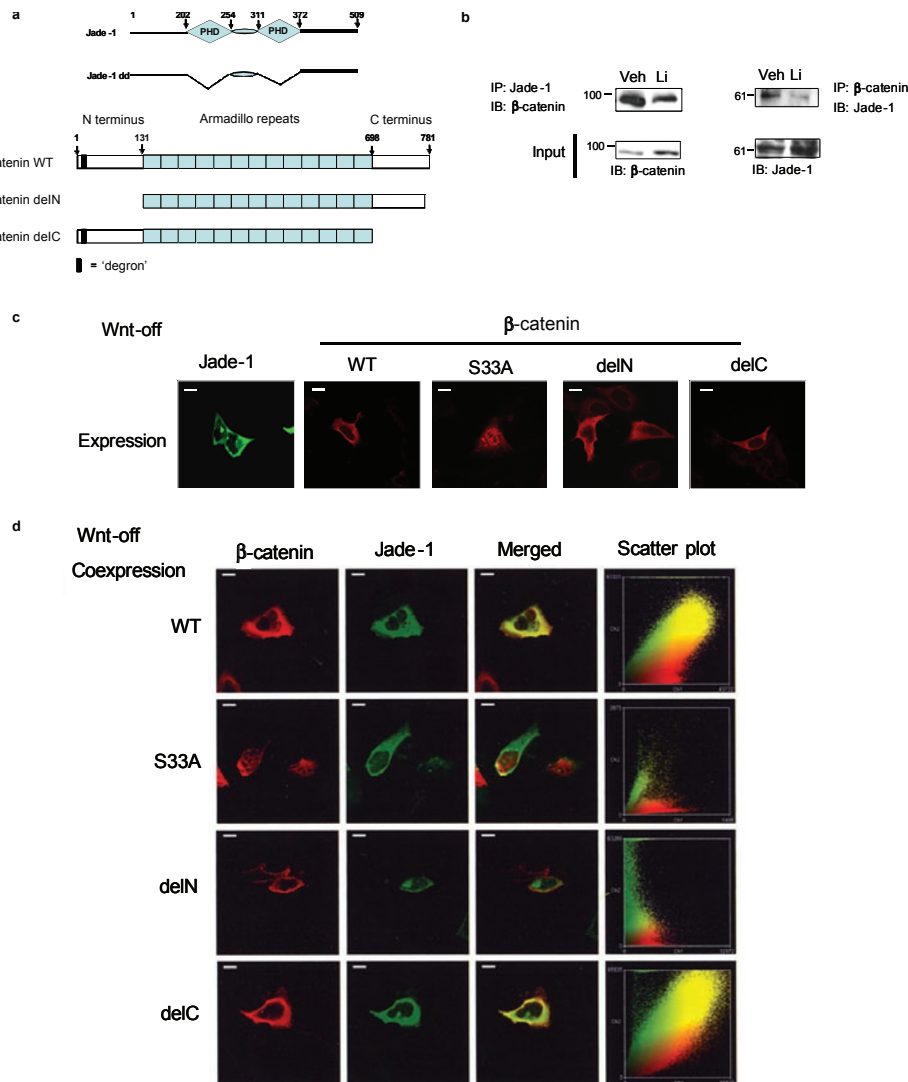


**Figure S1** Jade-1 directly binds  $\beta$ -catenin, and the interaction is enhanced in Wnt-off phase. **a**, Schematic of Jade-1 and  $\beta$ -catenin constructs. Jade-1 dd lacks both PHDs but has an intact inter-PHD region and contains aa 1-202, 254-311, and 372-509<sup>3,8</sup>.  $\beta$ -catenin constructs have an N-terminal Myc tag. **b**, Jade-1 binds to  $\beta$ -catenin in a Wnt-responsive manner. Immunoprecipitations were performed with WCLs of 293T cells pretreated with vehicle (water) (Veh) or 20 mM lithium chloride (Li) for 4 h using 1  $\mu$ g of either polyclonal Jade-1 antibody or pre-immune rabbit serum (data not shown).  $\beta$ -catenin was immunoprecipitated using monoclonal  $\beta$ -catenin antibody or isotype control (data not shown). Whole cell lysates (WCL) (10%) were probed for input. One of 2 similar experiments is shown. **c**, Expression of Jade-1 and  $\beta$ -catenin in Wnt-off phase. The 293 cells transfected with Flag-tagged Jade-1 or Myc-tagged  $\beta$ -catenin constructs pretreated with vehicle (PBS + 0.1% bovine serum albumin) for 4 h were processed for immunofluorescence. A single representative confocal image is shown. Wild-type  $\beta$ -catenin and the C terminus (delC) truncations of  $\beta$ -catenin localized to the cytosol and membrane. The N terminus (delN) truncation of  $\beta$ -catenin localized predominantly to the cytosol, while  $\beta$ -catenin S33A localized predominantly to the nucleus. Jade-1 localized to the cytosol and to lesser extent to the nucleus. Scale bar = 10  $\mu$ m. **d**, Jade-1 and  $\beta$ -catenin co-localize in Wnt-off phase. The 293 cells were transfected with Flag-tagged Jade-1 and Myc-tagged  $\beta$ -catenin constructs and pretreated with Wnt-3a (200 ng)

for 4 h. A single representative confocal image is shown. The co-localization was performed using the NIH ImageJ program in cells having comparable signal level for both constructs. Representative cells were analyzed. At least 15 confocal images comprising one Z-stack were generated for each cell. For the scatter plots, co-localization was performed using the entire Z-stack. Scatter plot points along the X or Y axis represent absence of co-localization, whereas scatter plot points along a diagonal represent co-localization. Scale bar = 10  $\mu$ m. **e**, Loss of Jade-1- $\beta$ -catenin co-localization in Wnt-on phase. The transfected 293 cells were pretreated with Wnt-3a (200 ng) for 4 h and processed as above. Scale bar = 10  $\mu$ m. **f**, Jade-1 preferentially binds phospho- $\beta$ -catenin in *in vitro* GST pull-down assays. (Left panels), GST beads or purified recombinant GST-tagged Jade-1 was incubated with cleaved, purified recombinant  $\beta$ -catenin (with or without *in vitro* phosphorylation). *In vitro* phosphorylation of  $\beta$ -catenin was performed by incubating GST-tagged  $\beta$ -catenin glutathione Sepharose beads with ATP and kinases CK1 and GSK-3 $\beta$  for 30 mins at 30  $^{\circ}$ C. The immunoblot was probed for  $\beta$ -catenin and phospho- $\beta$ -catenin. Ten percent of glutathione Sepharose beads was probed as input. (Right panels), GST beads or purified recombinant GST-tagged  $\beta$ -catenin was incubated with cleaved, purified recombinant Jade-1. Ten percent of GST beads was probed as input. Representative immunoblot of 3 experiments. G = GST, G-J = GST-Jade-1, G- $\beta$  = GST- $\beta$ -catenin, G-phospho $\beta$  = GST-phospho- $\beta$ -catenin, G-delN = GST- $\beta$ -catenin delN.

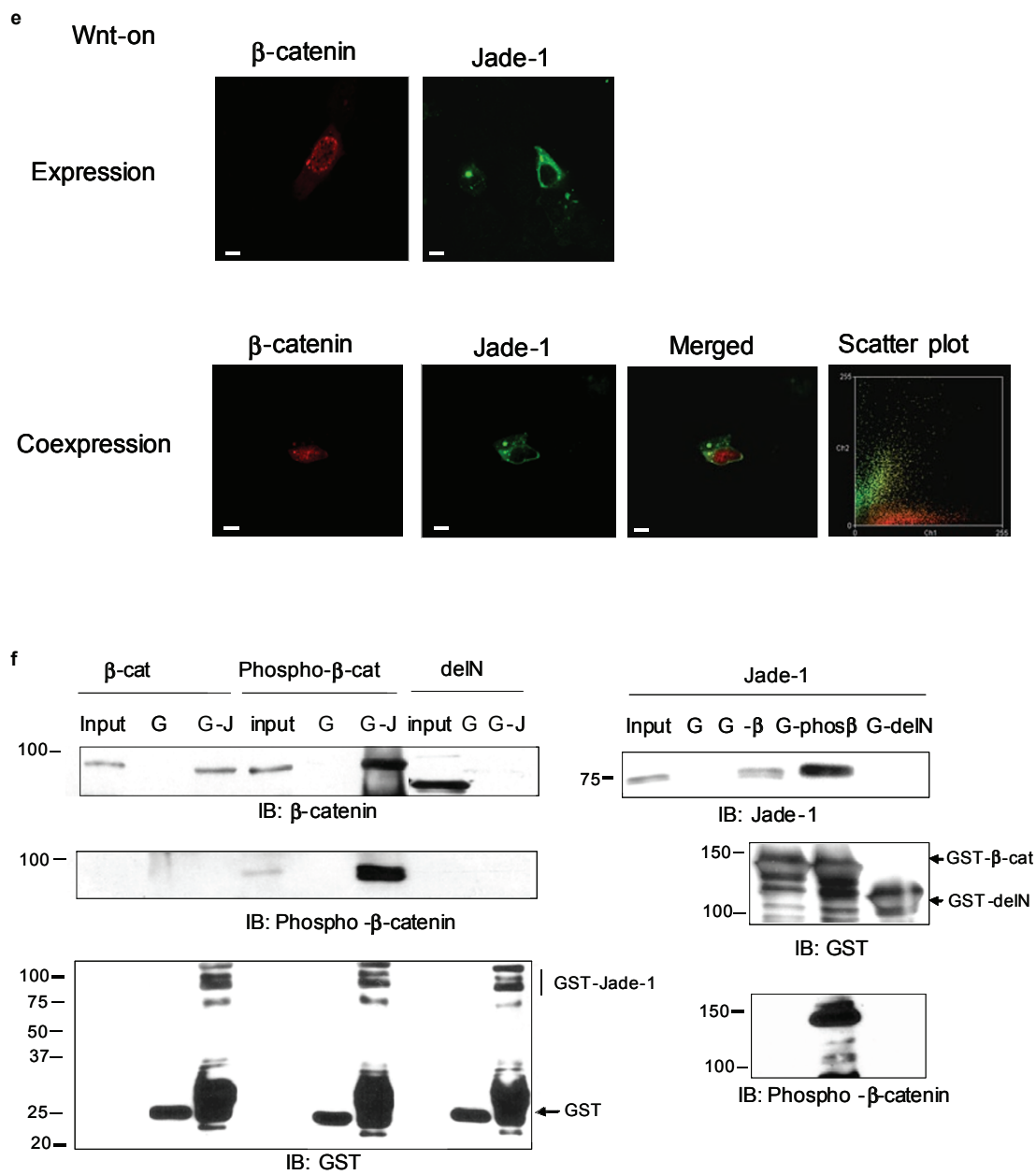
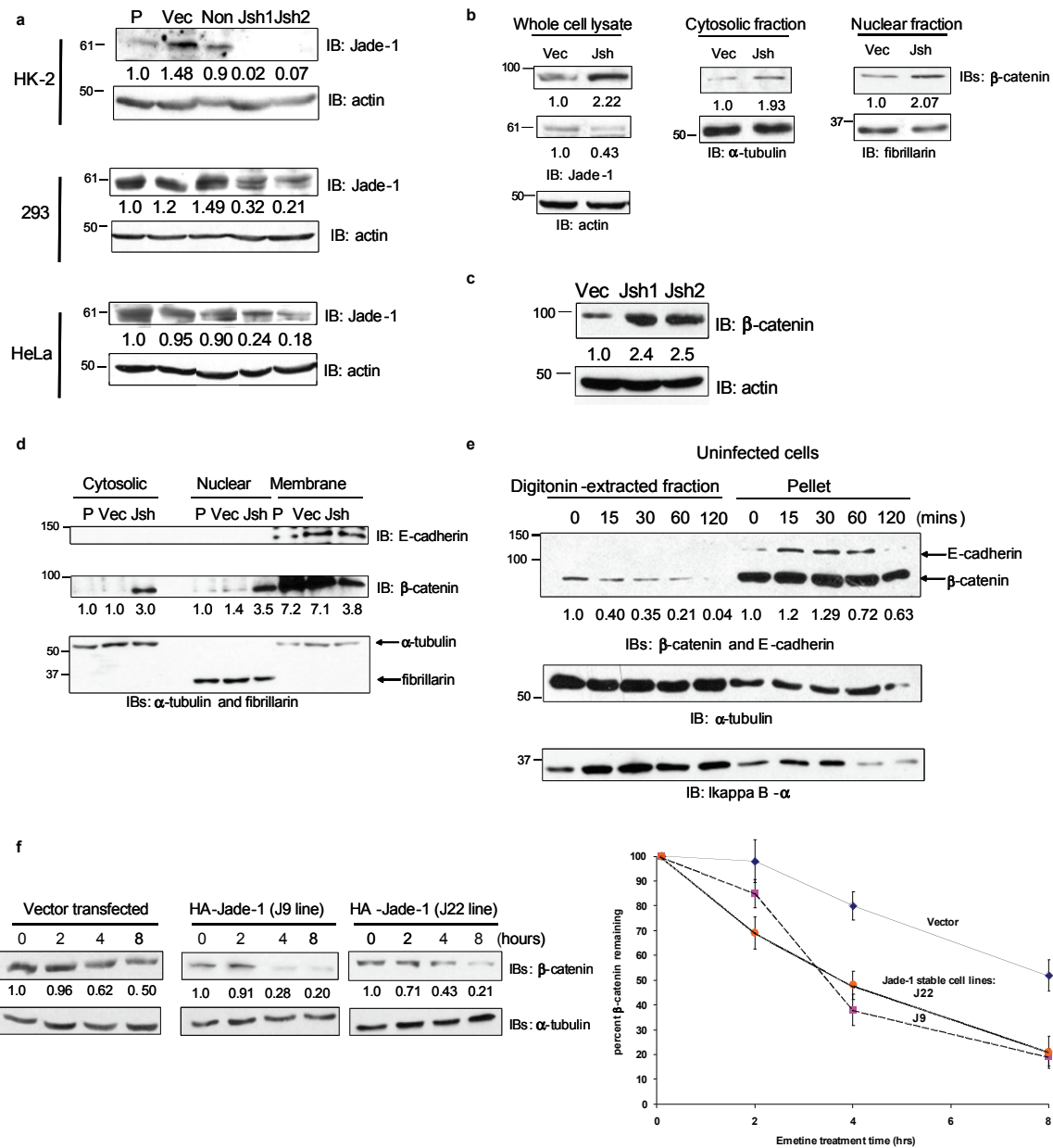
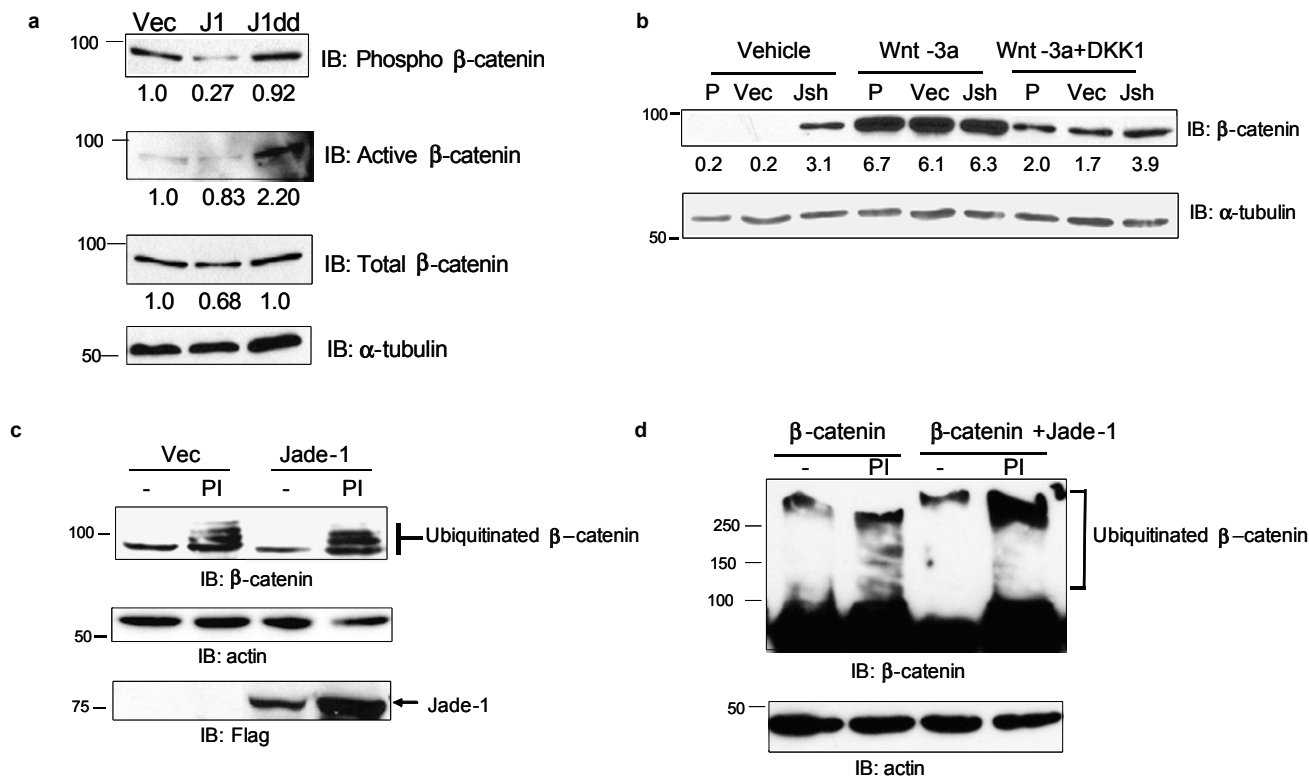


Figure S1 continued



**Figure S2** Jade-1 regulates endogenous  $\beta$ -catenin. **a**, *Jade-1* silencing by a lentiviral shRNA system in different cell lines. HeLa, 293 and HK-2 cell lines were infected with empty vector (Vec), non-silencing control (Non) or one of two *Jade-1* shRNA lentiviral vectors (Jsh). WCL from parental cells (P) or infected cells were probed for *Jade-1* and actin protein. Densitometry results are normalized to actin. One of two similar experiments is shown. **b**, *Jade-1* silencing by shRNA plasmid vector upregulates endogenous  $\beta$ -catenin. Extracts of empty vector (Vec) or *Jade-1* shRNA (JshRNA) plasmid vector transiently transfected 293T cells were probed for *Jade-1* and  $\beta$ -catenin protein. Representative immunoblot of three experiments. **c**, Endogenous  $\beta$ -catenin is upregulated with both *Jade-1* shRNA lentiviral constructs. Cytosolic protein extracts from HeLa cells infected with one of two lentiviral *Jade-1* shRNA constructs (Jsh1 or Jsh2) were probed for  $\beta$ -catenin. One of two similar experiments is shown. **d**, *Jade-1* silencing increases the cytosolic and nuclear fractions but not the membrane fraction of  $\beta$ -catenin. Extracts of parental HK-2 cells (P) or cells infected with empty vector (Vec) or *Jade-1* shRNA lentivirus (Jsh) were subjected to cell fractionation. Cytosolic, nuclear and membrane fractions were probed for  $\beta$ -catenin.  $\alpha$ -tubulin, fibrillarin and E-cadherin served as loading controls

and markers of cytosolic, nuclear and membrane fractions, respectively. These control blots were generated by cutting the membrane at the expected molecular weights of the controls and immunoblotting separately. One of two similar experiments is shown. **e**, The digitonin-extracted fraction is enriched for cytosol and devoid of membrane contamination. Equal amounts of protein from the digitonin-extracted fractions of 293 cells pretreated with protein translation inhibitor emetine (20  $\mu$ M), harvested at different time points, were probed for  $\beta$ -catenin. E-cadherin served as a marker for the membrane fraction, and  $\alpha$ -tubulin and I $\kappa$ B- $\alpha$  served as markers of cytosol. These control blots were generated by cutting the membrane at the expected molecular weights of the controls and immunoblotting separately. One of two similar experiments is shown. **f**, *Jade-1* expression destabilizes  $\beta$ -catenin in renal cancer cells. Cytosolic fractions from clonal 786-O cell lines stably expressing empty vector or *Jade-1* (J9, J22)<sup>4,5</sup> harvested after 20  $\mu$ M emetine treatment were probed for  $\beta$ -catenin. Percent  $\beta$ -catenin remaining was analyzed by densitometry after normalizing to  $\alpha$ -tubulin.  $\beta$ -catenin half-life was reduced from 8 hrs to 3.5 hrs in the *Jade-1*-expressing 786-O cell lines. Graph shows mean result of three experiments. Error bars = SEM.



**Figure S3** Jade-1 preferentially regulates endogenous phospho-β-catenin in Wnt-off phase and enhances proteasomal degradation of β-catenin. **a**, Jade-1 downregulates total endogenous β-catenin by reducing predominantly phospho-β-catenin. Cytosolic protein extracts from 293T cells transiently transfected with full-length Myc-tagged Jade-1 (J1) or Jade-1 dd (J1dd) were probed for total β-catenin. The membrane was stripped and reprobed for phospho-β-catenin (β-catenin phosphorylated at serine 33, 37 and threonine 41) and active β-catenin (non-phosphorylated at serine 37 and threonine 41). Cytosolic fractions were probed for the Myc tag to confirm equivalent expression of Jade-1 and Jade-1 dd (data not shown). One of two similar experiments is shown. **b**, Jade-1 regulation of β-catenin during Wnt-on and Wnt-off phase. HK-2 parental cells (P) or

cells infected with empty vector (Vec) or *Jade-1* shRNA (Jsh) lentivirus were treated for 4 h with Wnt-3a (200 ng), with or without DKK1 (200 ng). The cytosolic fractions were probed for β-catenin and α-tubulin. Representative immunoblot of three experiments. **c**, Proteasome inhibitor treatment abrogates the effect of endogenous Jade-1 on β-catenin. Transfected 293T cells were incubated with proteasome inhibitor (PI) MG132 at 10 μM for 12 hrs. WCL were probed with β-catenin, α-tubulin or Flag-tag antibodies. One of two similar experiments is shown. **d**, Jade-1 increases accumulation of high molecular weight polyubiquitinated β-catenin in the presence of PI. The 293T cells transiently transfected with Jade-1 and β-catenin were treated with PI MG132 at 10 μM for 12 h. WCL were probed as shown. One of two similar experiments is shown.

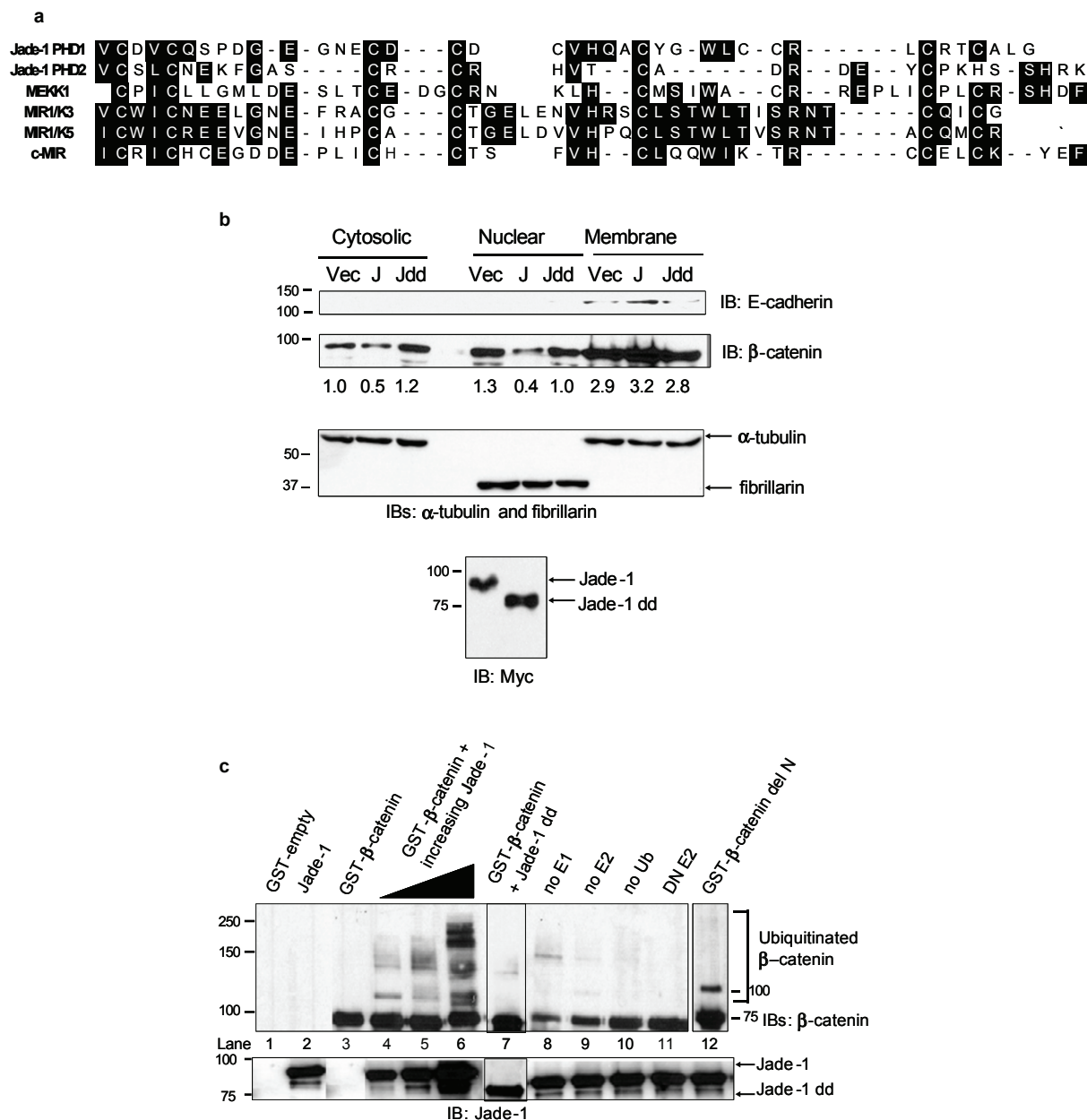


**Figure S4** Jade-1 ubiquitinates  $\beta$ -catenin. **a**, The PHDs of Jade-1 align well with the PHDs of proteins with known E3 ubiquitin ligase activity. The MacVector (Accelrys) sequence analysis program was used to align the PHDs of human Jade-1, MEKK1 (Q13233), viral MIR1 (K3), MIR2 (K5) (U93872) and c-MIR (hCP36279). **b**, Full-length Jade-1, but not Jade-1 dd, reduces abundance of the cytosolic and nuclear fractions of  $\beta$ -catenin. Protein extracts of 293T cells transiently transfected with full-length Jade-1 (J1) or Jade-1 dd (J1dd) were probed for  $\beta$ -catenin.  $\alpha$ -tubulin, fibrillarin or E-cadherin served as loading controls and markers of cytosolic, nuclear and membrane fractions, respectively. These control blots were generated by cutting the membrane at the expected molecular weights of the controls and immunoblotting separately. Cytosolic fractions were probed to examine

expression of Jade-1 and Jade-1 dd. One of two similar experiments is shown. **c**, Dose-dependent *in vitro* ubiquitination of  $\beta$ -catenin by Jade-1. Ubiquitination reactions were reconstituted by incubating GST- $\beta$ -catenin beads with E1 activating enzyme, E2 conjugase (UbcH6), E3 ligase Jade-1 (in increasing amounts, 250, 750, or 1200 nM) or Jade-1 (full-length or dd) (750 nM), Myc-tagged human recombinant ubiquitin (Ub) and MgCl<sub>2</sub>-ATP. No E1, no E2, no Ub and DN E2 reactions served as negative controls.  $\beta$ -catenin ubiquitination was detected using polyclonal  $\beta$ -catenin C-terminal antibody. Reactions without E1, E2, or ubiquitin, or with dominant-negative (DN) UbcH6, served as negative controls (lanes 8-11). Jade-1 input was detected by immunoblot. Lane 7 was rearranged from the same blot. One of two similar experiments is shown.

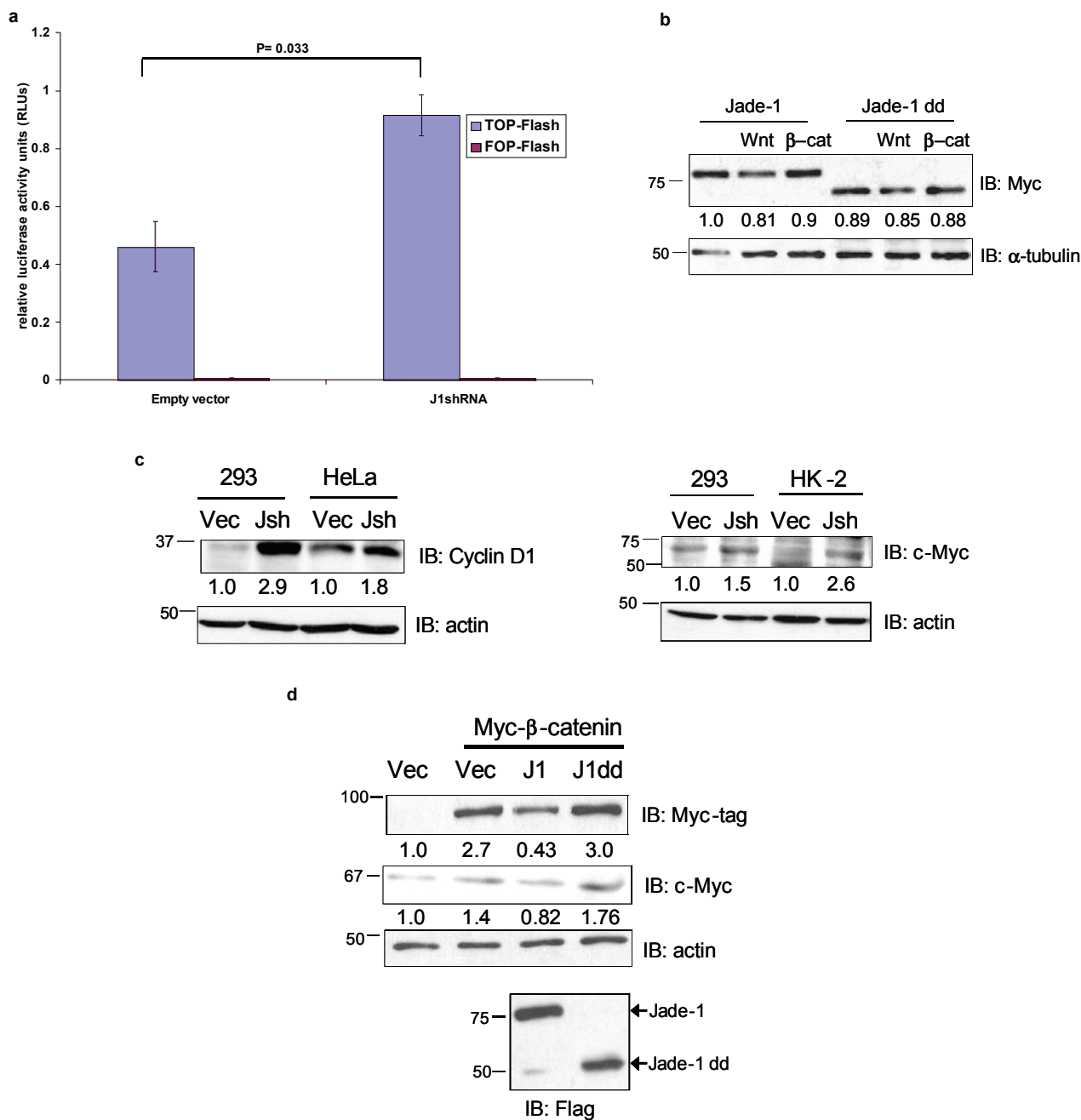


**Figure S5** *Jade-1* regulates  $\beta$ -catenin transcriptional target genes. **a**, *Jade-1* silencing results in a significant spontaneous endogenous Wnt activity. The 293 cells stably infected with empty vector or *Jade-1* shRNA lentiviral vectors were transiently transfected with TOP-Flash or FOP-Flash and *Renilla* luciferase vectors. Activity of the Wnt signaling pathway was quantified by measuring relative firefly luciferase activity units (RLUs) normalized to *Renilla* luciferase. Mean results of three experiments are shown. Error bars = SEM. Student's t-test was applied to determine statistical significance,  $p = 0.033$ . **b**, Comparable expression of Myc-tagged *Jade-1* and *Jade-1* dd protein in *Xenopus laevis* embryos injected also with capped mRNAs for *Xwnt-8* or  *$\beta$ -catenin*. Embryos were harvested

at stage 10, and the extracts were resolved by SDS-PAGE. The membrane was probed using Myc and  $\alpha$ -tubulin antibodies. **c**, Endogenous Wnt targets are upregulated in *Jade-1* silenced cell lines. WCL from cells infected with empty vector or from *Jade-1* silenced cells were probed for cyclin D1 or c-Myc. Representative immunoblot of four experiments. **d**, Full-length *Jade-1*, but not *Jade-1* dd, downregulates endogenous c-Myc. Whole cell extracts of 293T cells transfected with Myc-tagged  $\beta$ -catenin with or without Flag-*Jade-1* or Flag-*Jade-1* dd were probed with c-Myc antibody detecting endogenous c-Myc protein. Flag- and Myc-tag antibodies were used to detect transfected Flag-tagged *Jade-1* and Myc-tagged  $\beta$ -catenin, respectively. One of two similar experiments is shown.

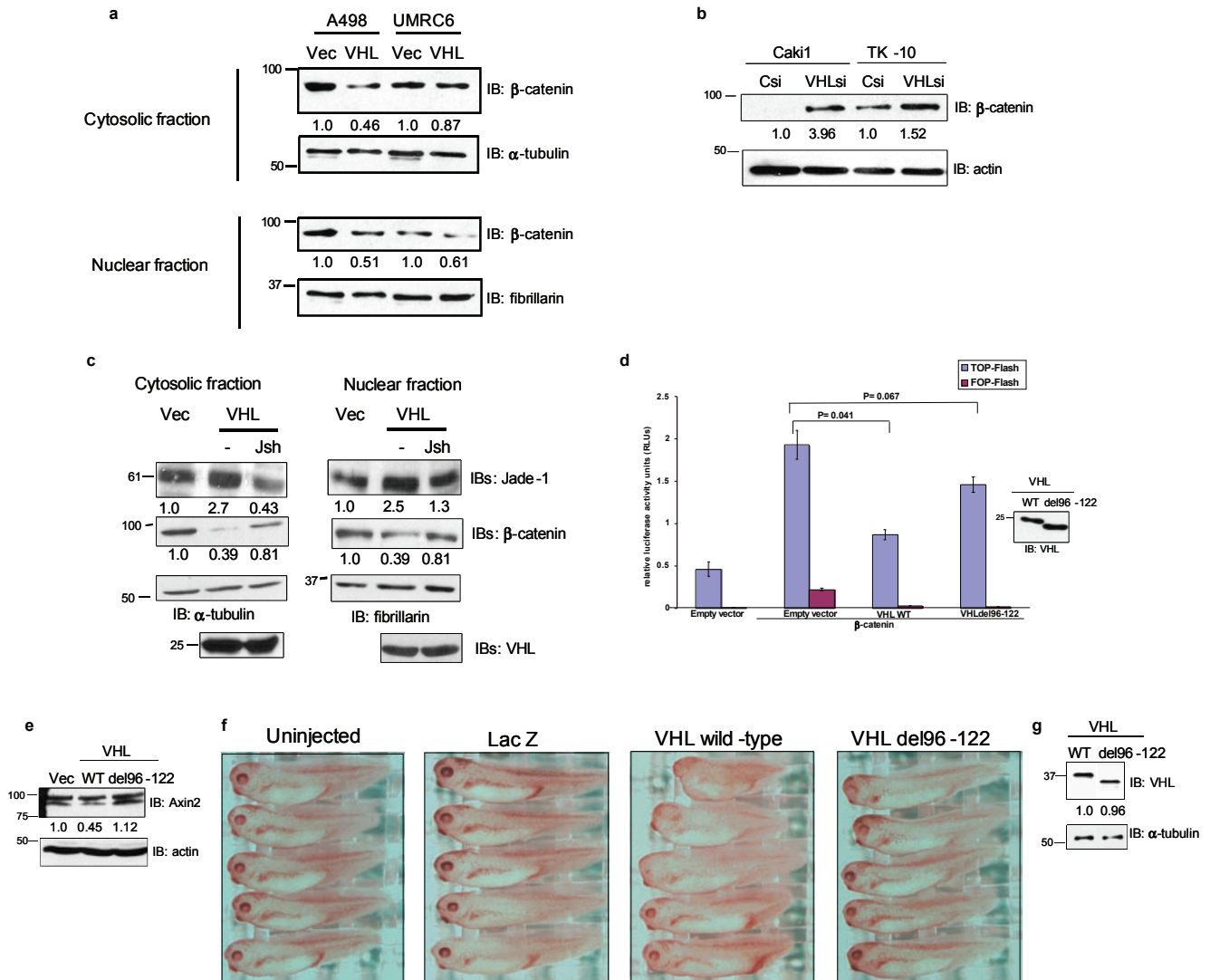


**Figure S6** pVHL regulates  $\beta$ -catenin through Jade-1. **a**, pVHL downregulates endogenous  $\beta$ -catenin. Fractions of *VHL*-deficient renal cancer cell lines stably expressing pVHL were probed. The UMR6 cell line has a lower level of expression of pVHL compared to the A498 cell line (data not shown). One of two similar experiments is shown. **b**, pVHL knock-down increases endogenous  $\beta$ -catenin. Cytosolic fractions of *VHL*-intact renal cancer cell lines transfected with control (Csi) or *VHL* siRNA (VHLsi) oligonucleotides were probed for  $\beta$ -catenin. One of two similar experiments is shown. **c**, *Jade-1* silencing in the presence of pVHL mitigates  $\beta$ -catenin regulation. The 293T cells were transiently transfected as shown. pVHL was detected using monoclonal pVHL antibody. One of two similar experiments is shown. **d**, Wild-type pVHL, but not pVHL del96-122, suppresses  $\beta$ -catenin-mediated transcriptional activation. The 293T cells transiently transfected with empty vector or  $\beta$ -catenin; wild-type pVHL, pVHL del96-122 or empty vector; and TOP-Flash or FOP-Flash were subjected to luciferase assay. Mean results of three experiments are shown. Error bars = SEM.  $p = 0.041$  (\* = statistically significant),  $p = 0.067$  (NS) by Student's t-test. **e**, Wild-type pVHL, but not pVHL del96-122, suppresses Axin2. WCL of 293T cells transfected with empty vector (Vec), wild-type pVHL (WT) and pVHL del96-122 (del96-122) were immunoblotted

for Axin2 and actin. One of two similar experiments is shown. **f**, Wild-type pVHL, but not pVHL del96-122, significantly inhibits endogenous axis in *Xenopus laevis* embryos. *In vitro* transcribed capped *LacZ* (0.145-0.288 ng) (N = 73), wild-type *VHL* (0.130-0.194 ng) (N = 115) or *VHL del96-122* (0.146-0.293 ng) (N = 100) mRNA was injected into dorsal blastomeres of *Xenopus laevis* embryos. Uninjected (N = 135) and *LacZ* injected embryos served as controls. In uninjected embryos, normal dorsoanterior index (DAI) = 96%, partial axis duplication = 3% of embryos. In *LacZ* injected embryos, normal DAI = 92%, DAI 3-4 = 3%, gastrulation defects (GD) = 3%, partial axis duplication = 3% of embryos. In wild-type *VHL* injected embryos, normal DAI = 49%, DAI 3-4 = 30%, DAI 0-2 = 5%, GD = 12% and partial double axis = 3% of embryos. In del96-122VHL injected embryos, normal DAI = 75%, DAI 3-4 = 15%, DAI 0-2 = none, GD = 7%, partial axis duplication = 3% embryos. Wild-type pVHL suppressed endogenous axis formation significantly more than pVHL del96-122 (Chi square test,  $p = 0.0046$ ). Six experiments were performed. **g**, Comparable expression of Myc-tagged pVHL wild-type and pVHL del96-122 protein in *Xenopus laevis* embryos. *Xenopus laevis* embryos injected with capped mRNAs were harvested at stage 10. Protein extracts were resolved by SDS-PAGE. Representative immunoblot of six experiments.



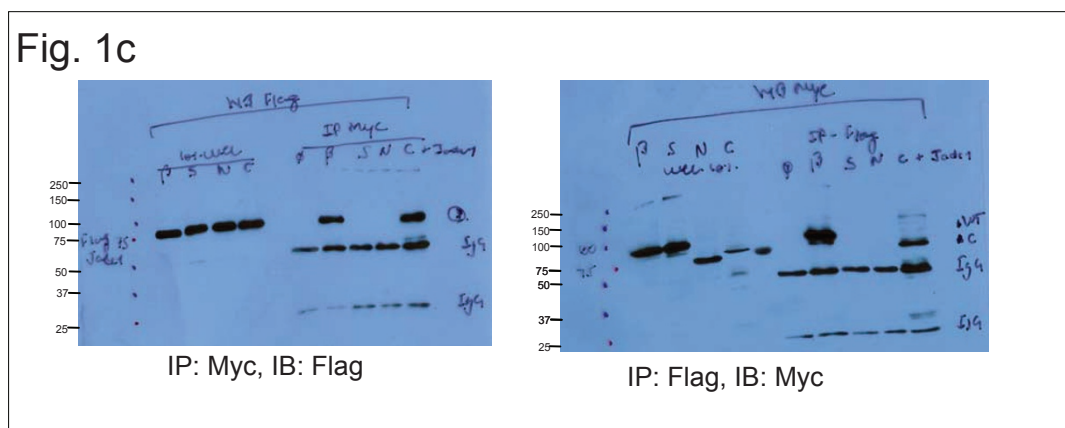
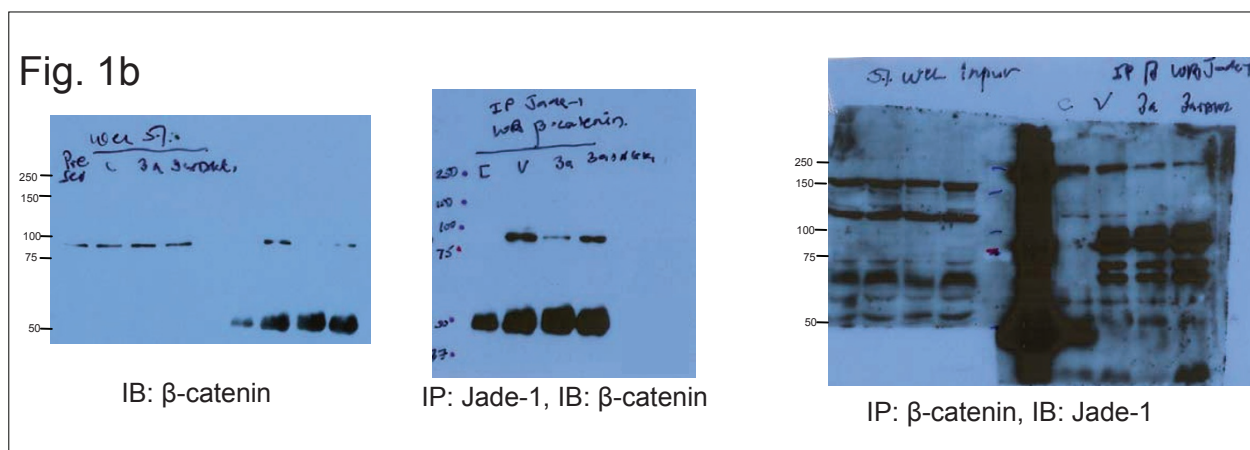
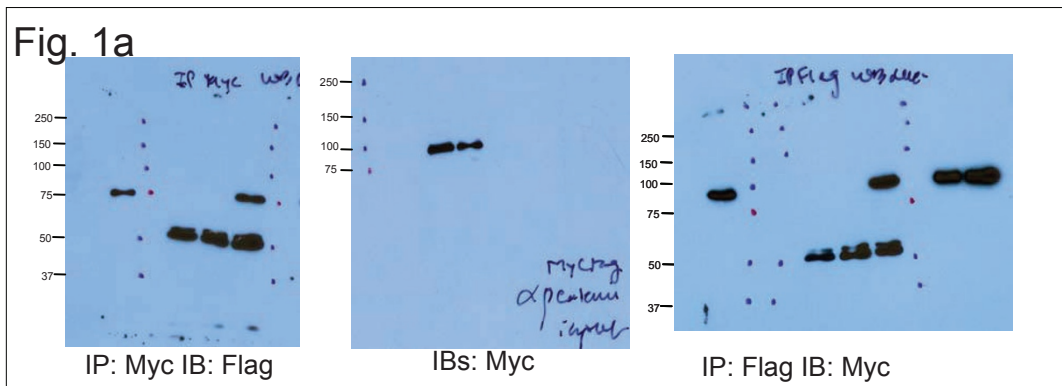


**Figure S7** Complete scans of immunoblots and RT-PCR gels. For each panel the corresponding figure shown in the paper is indicated on top. Position of molecular size markers (in kD) is also shown.

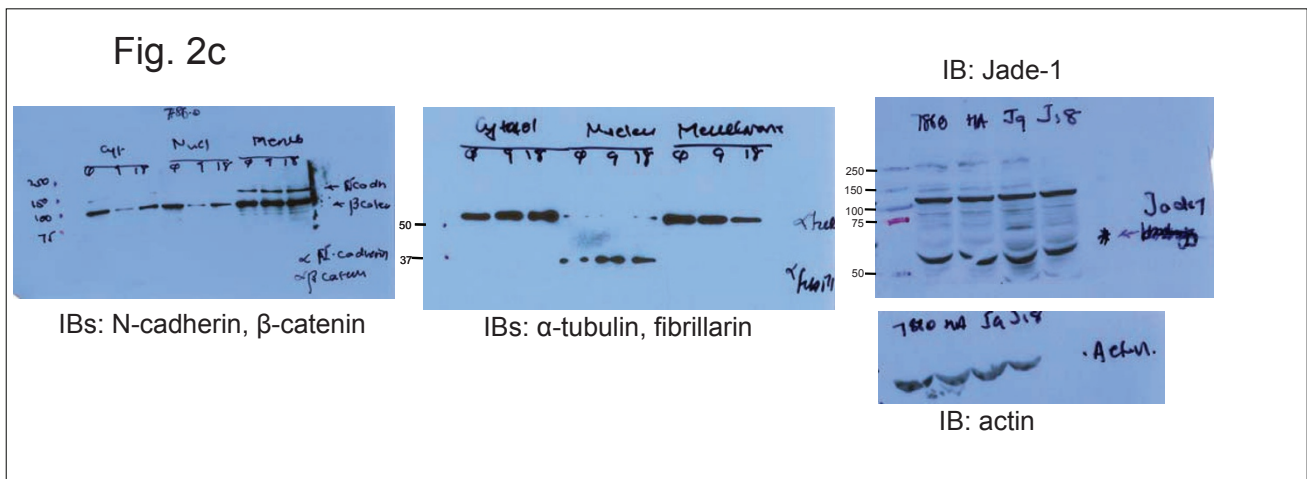
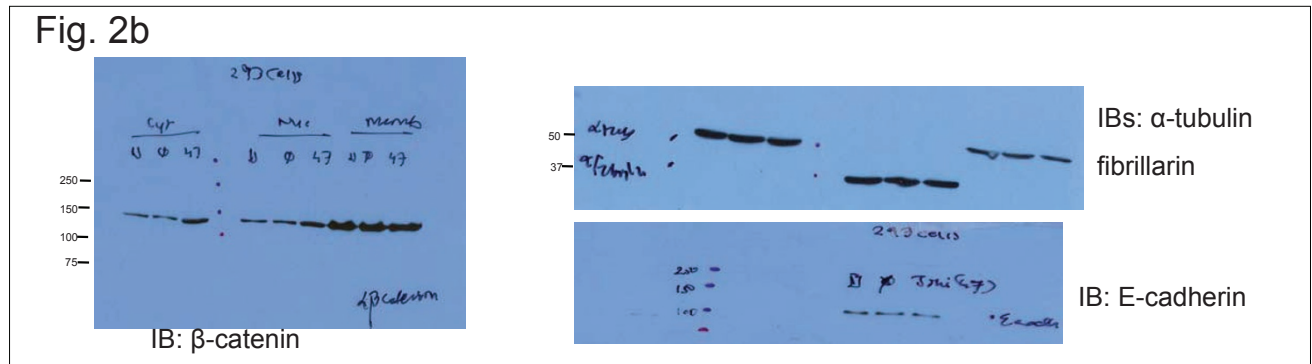
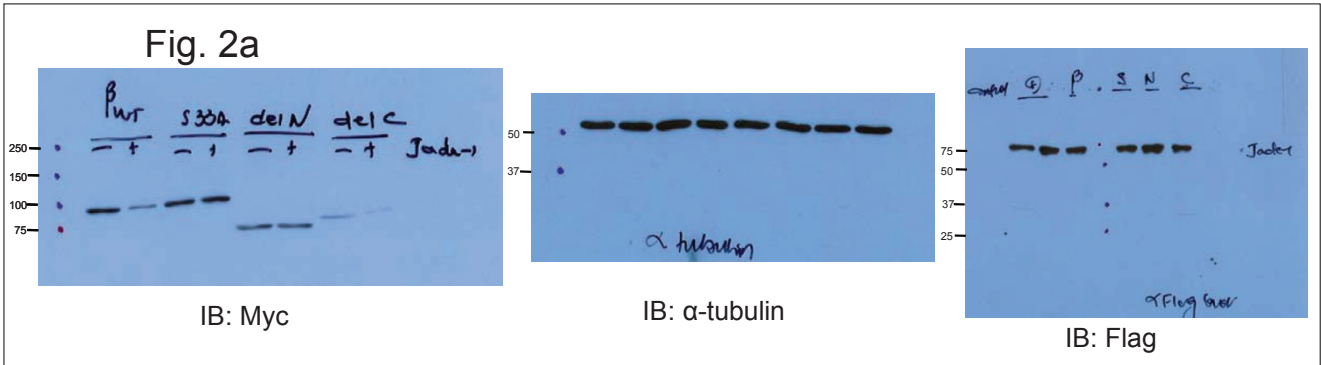


Figure S7 continued

Fig. 2d

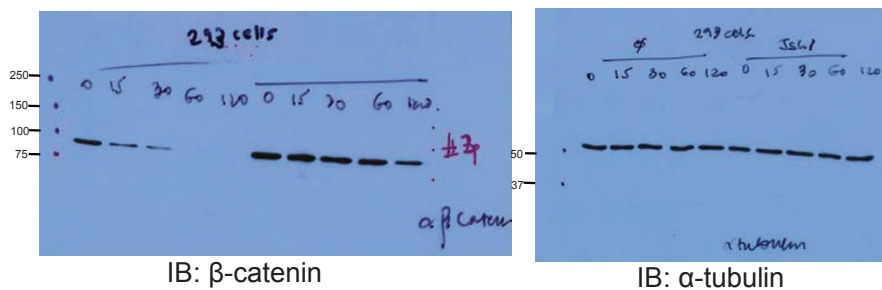


Fig. 2e

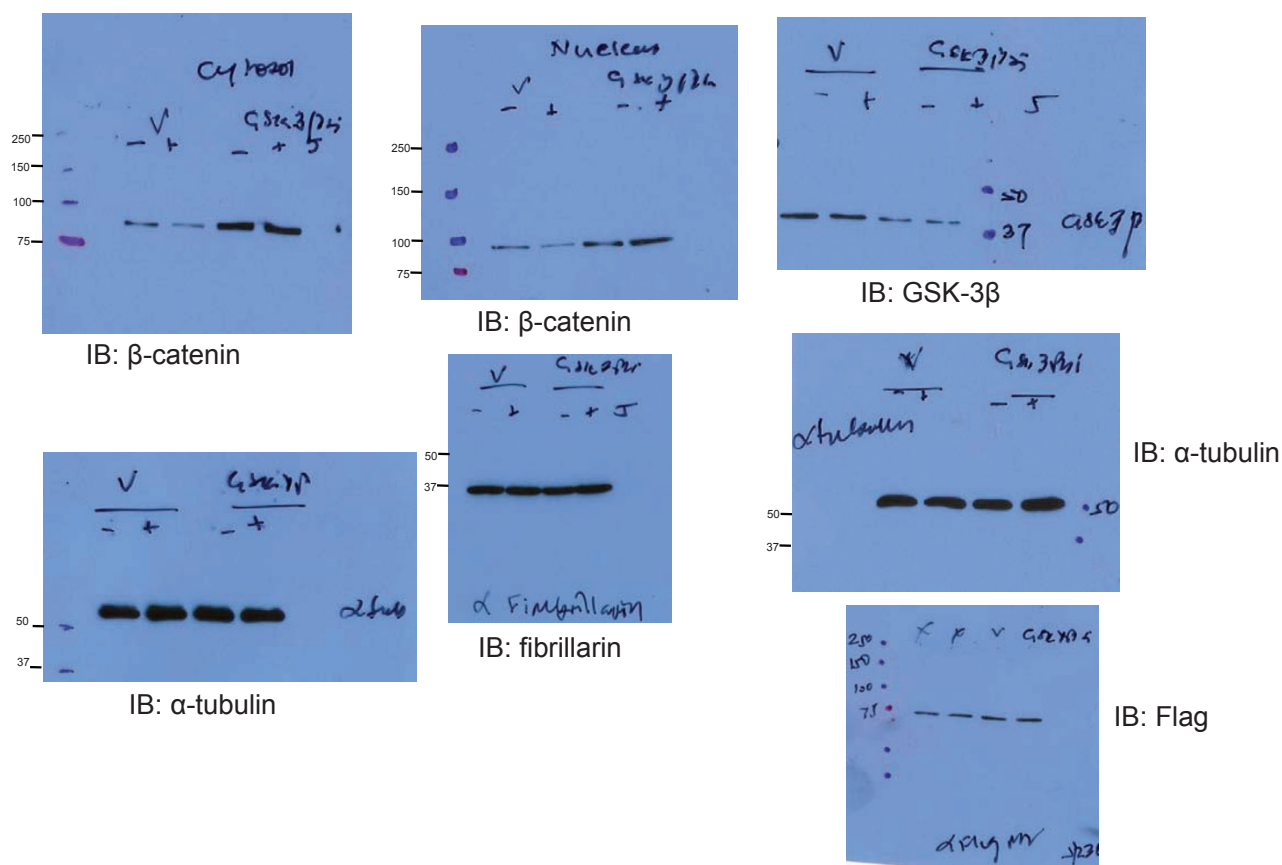


Figure S7 continued

Fig. 2f

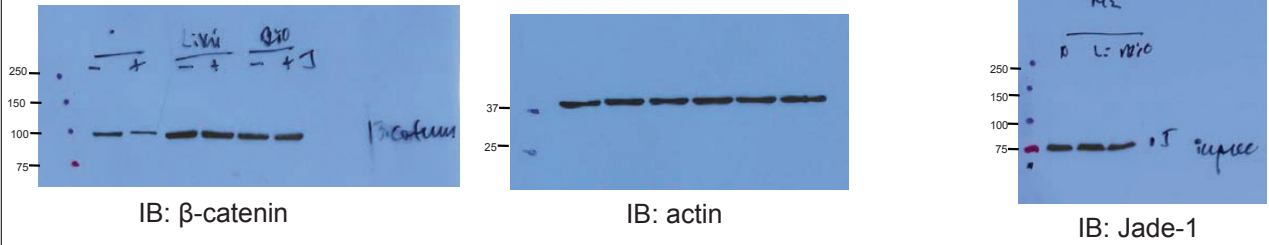


Fig. 2g

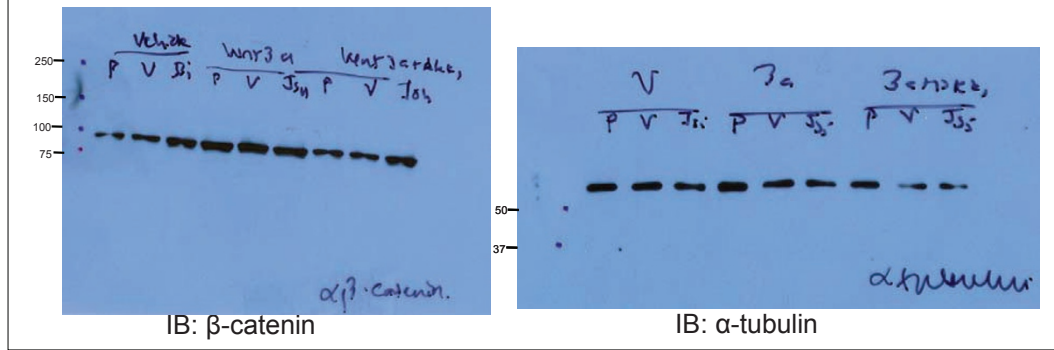


Figure S7 continued

Fig. 3a

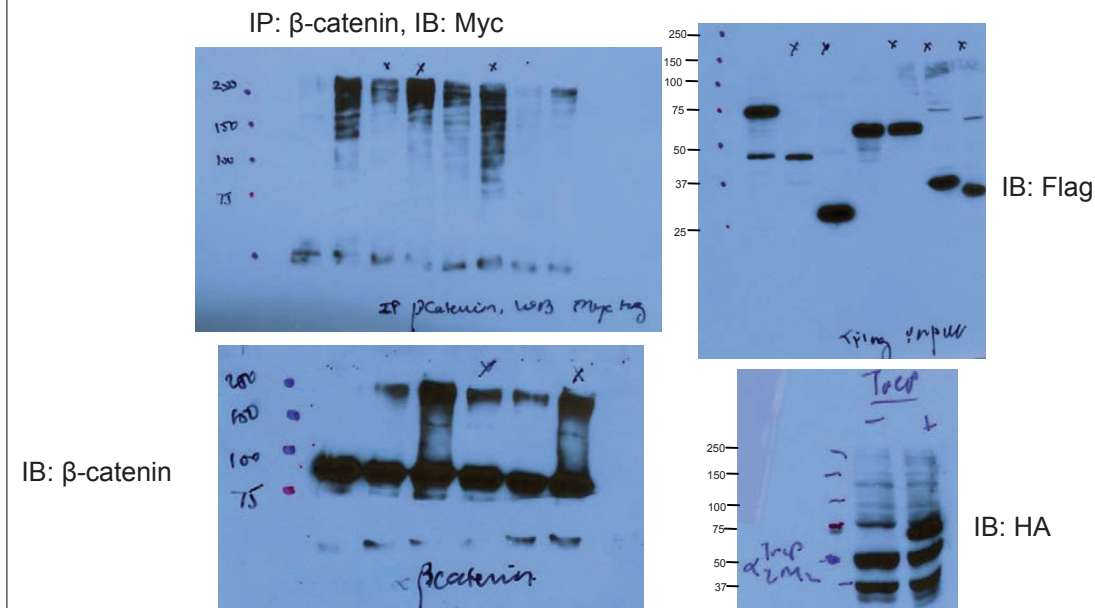


Fig. 3b

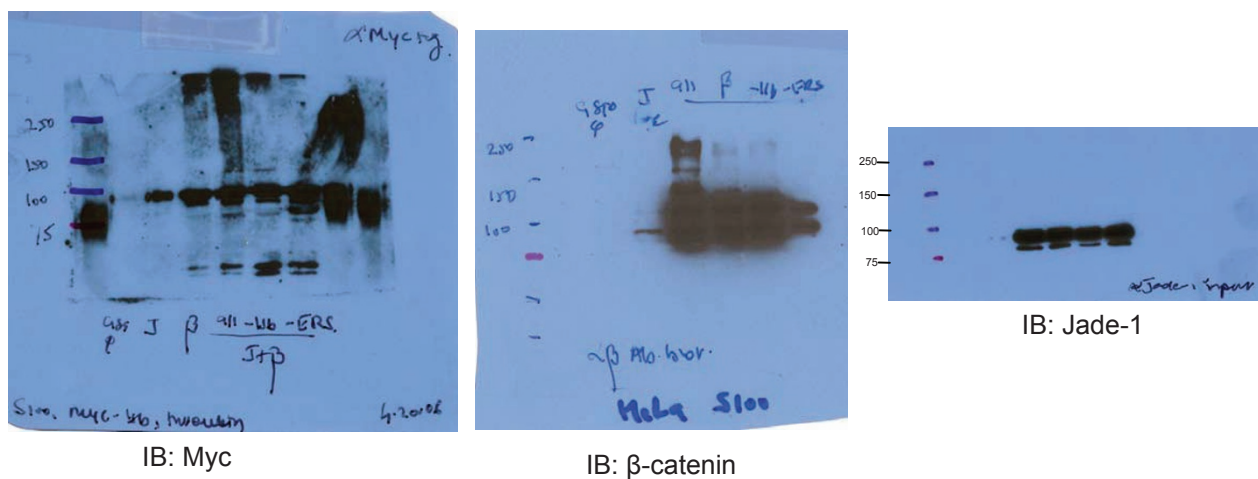


Figure S7 continued

Fig. 3c

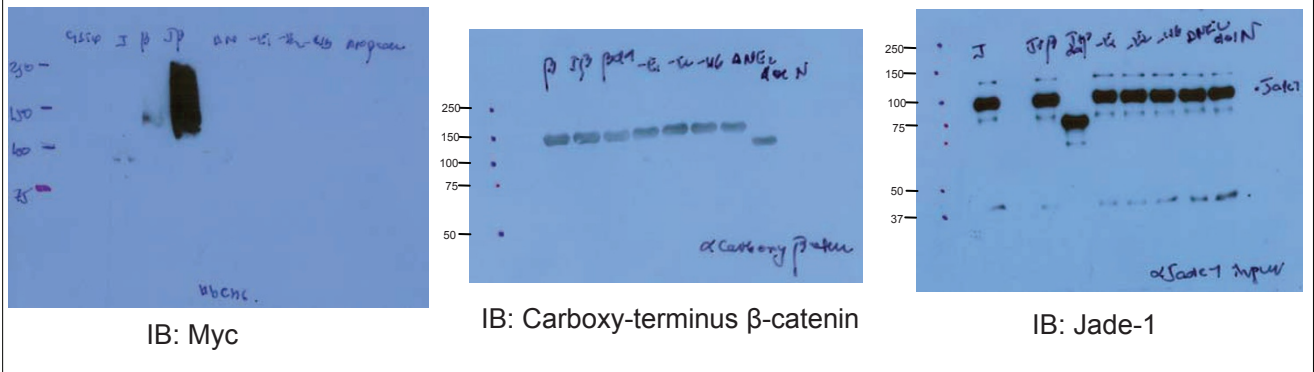


Fig. 3d

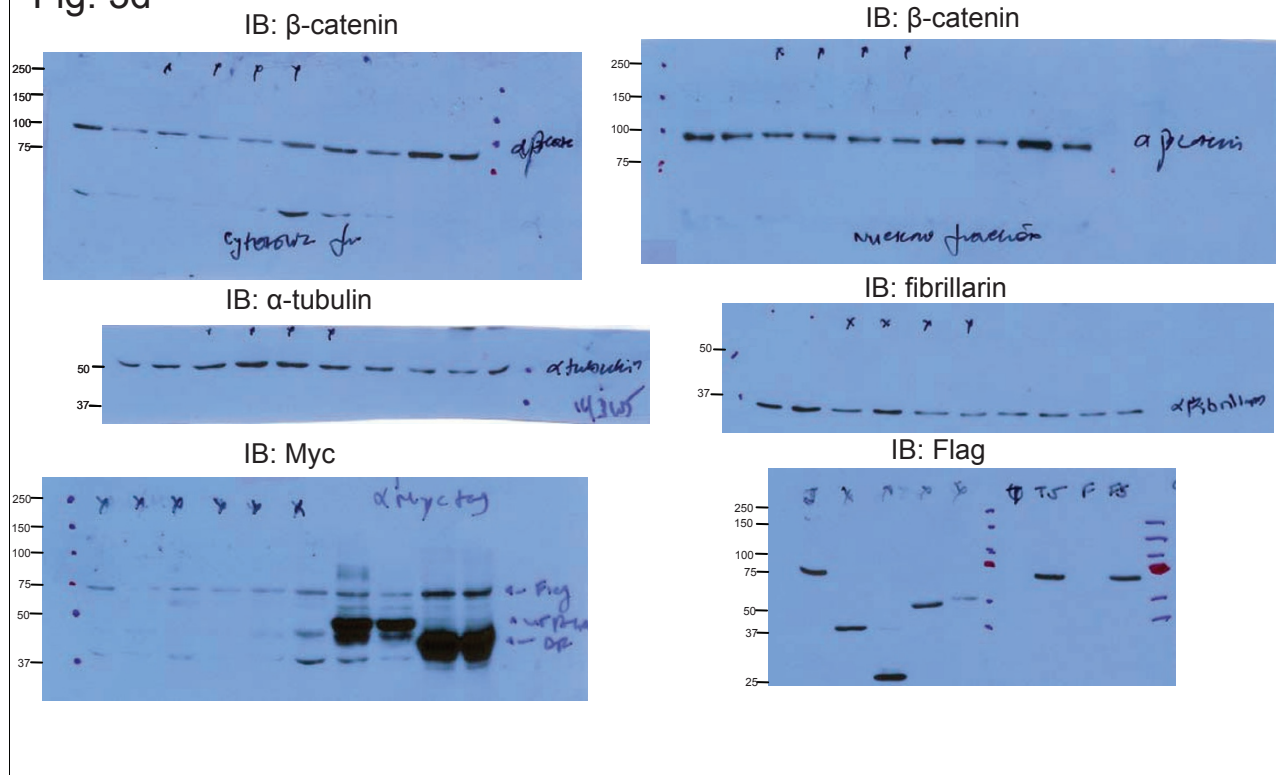


Figure S7 continued

Fig. 4a

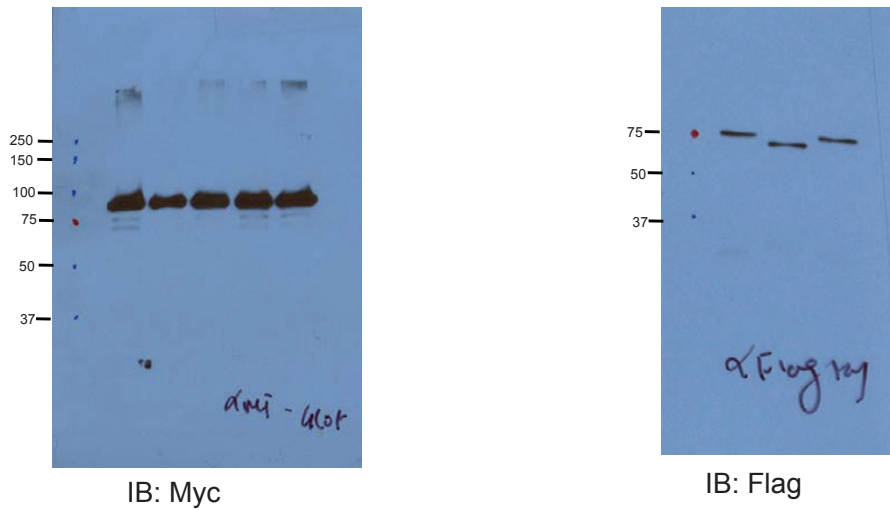


Fig. 4d

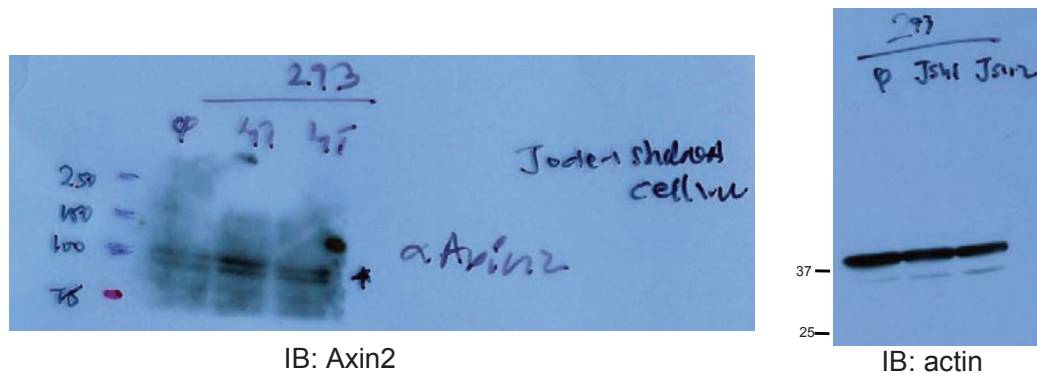


Figure S7 continued

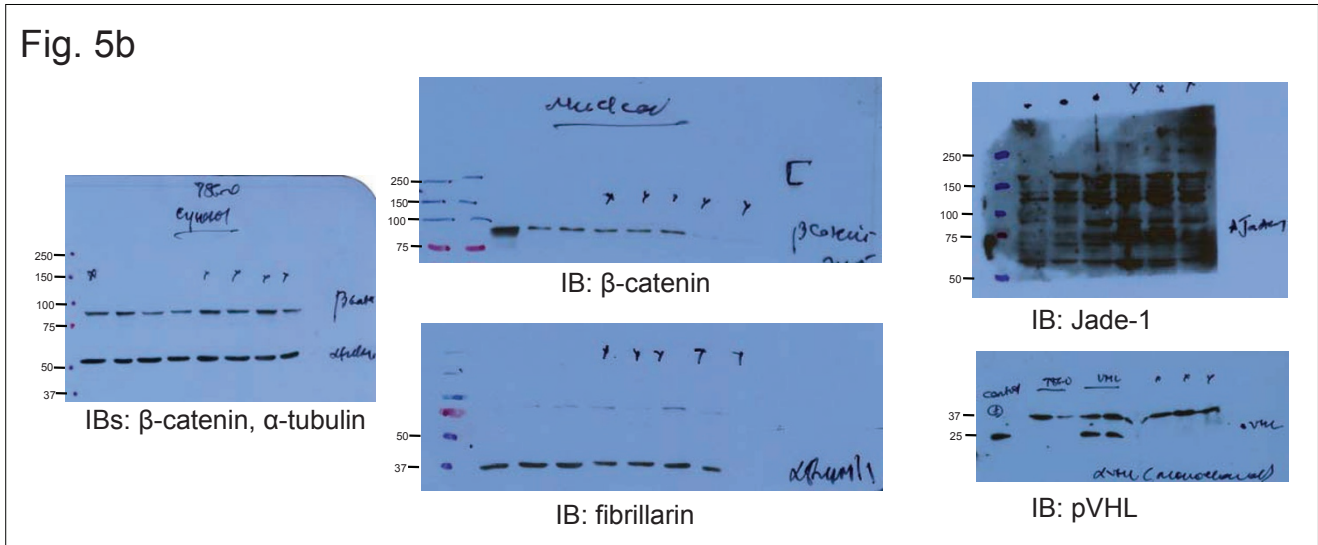
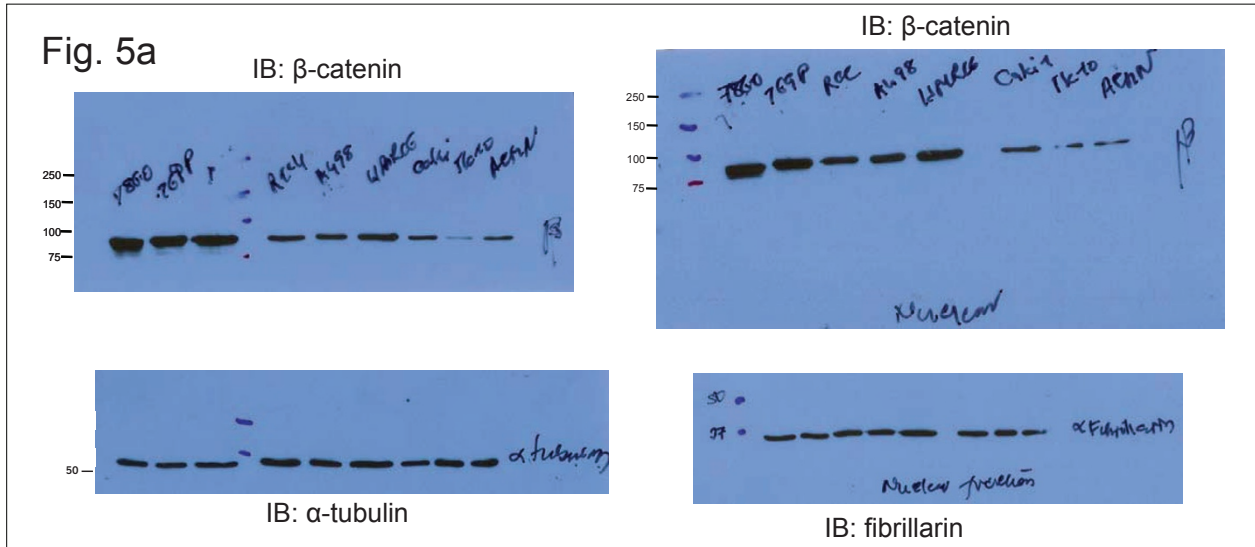


Figure S7 continued



Fig. 5c

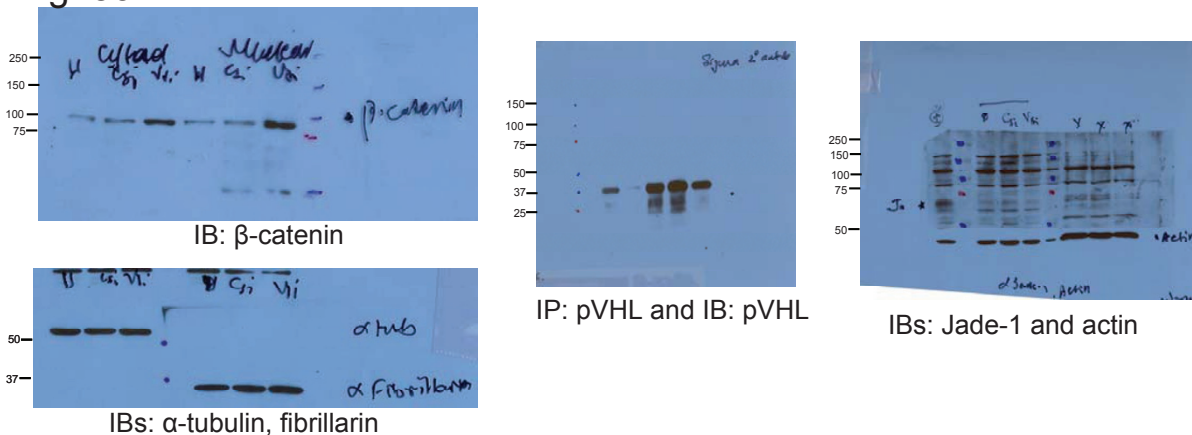


Fig. 5d

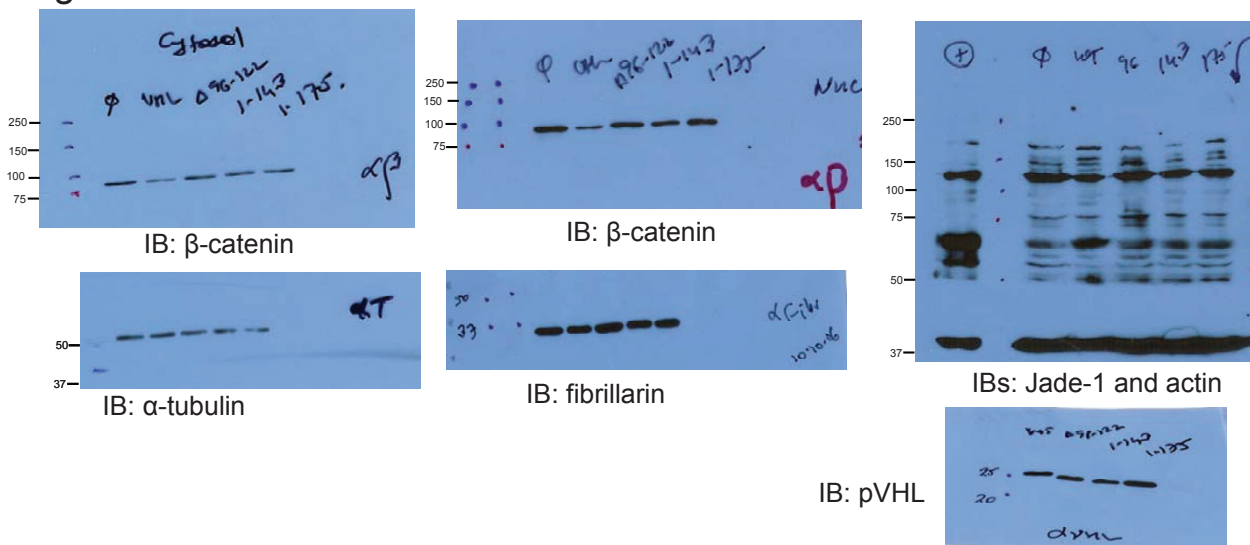


Figure S7 continued

Fig. 5e

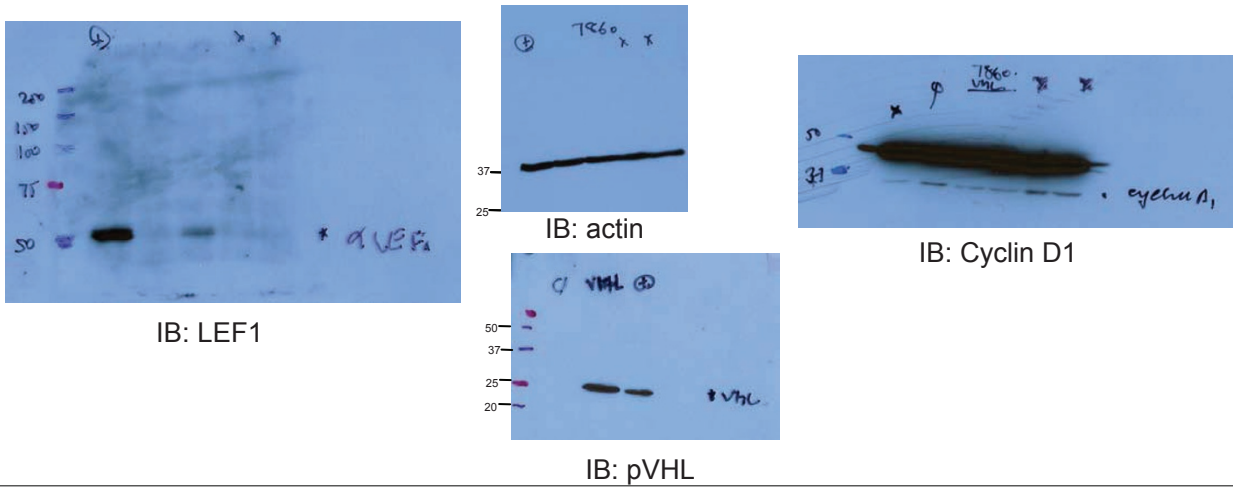


Fig. 5f

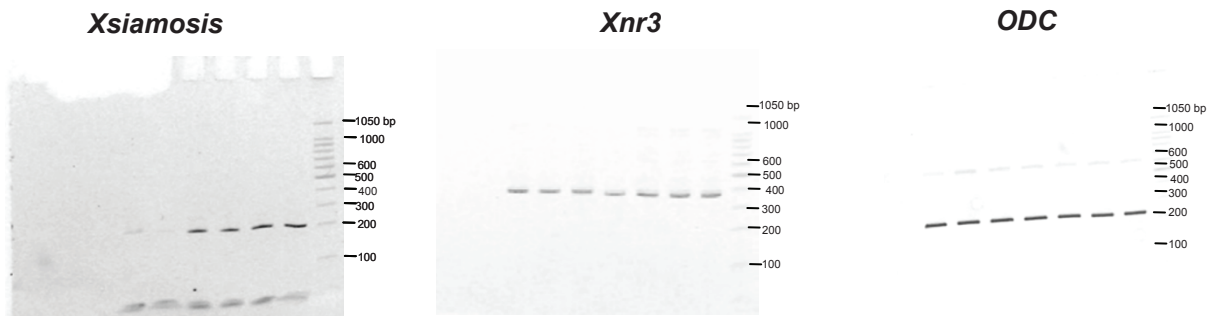


Figure S7 continued

## Supplementary Methods

**Cell culture, transfections and chemical treatment.** The 293, 293T, 786-O, 769-P, RCC4, A498, UMRC6, Caki1, TK-10 and ACHN cell lines were grown as described previously<sup>4,5</sup>. Cultured cells plated overnight were transiently transfected using Lipofectamine 2000 (Invitrogen) per manufacturer instructions. Lithium chloride (Sigma) and 6-bromoindirubin-3'-oxime (BIO) (Calbiochem) were used to inhibit GSK-3 $\beta$  activity. Human recombinant Wnt-3a and DKK-1 dissolved in PBS + 0.1% bovine serum albumin were obtained from R & D Systems.

**Constructs.** Flag-tagged Jade-1 wild-type and Jade-1 lacking both PHDs (Jade-1 dd) in pFlag-CMV2 vector have been described previously<sup>3</sup>. Wild-type human Myc-tagged  $\beta$ -catenin was cloned into *Xenopus* expression vector pCS2+. Myc-tagged ubiquitin in pCMV2 vector was a gift from Z.-X. Xiao (Boston University). Constitutively active (CA)  $\beta$ -catenin S33A (amino acid substitution at GSK-3 $\beta$  phosphorylation site) in pCS2+MMBcmyc-tag vector and  $\beta$ -catenin delN (aa 131-781) in pGEX2T were kindly provided by R. Kemler (Max-Planck Institute for Immunobiology, Germany). Human  $\beta$ -catenin C and N terminus deletion constructs (delC and delN) in pBAT expression vector were generous gifts from W. Birchmeier (Max-Delbruck-Center for Molecular Medicine, Germany). TOP-Flash and FOP-Flash constructs were gifts from B. Vogelstein (Johns Hopkins University).  $\beta$ -TrCP wild type and dominant negative (DN) in pcDNA3.1 myc/His vector were gifts from R. Benarous (Institute Pasteur, France). HA-tagged  $\beta$ -TrCP wild-type was a gift from S. C. Sun (Penn State University). *GSK-3 $\beta$*  shRNA plasmid (pKD-GSK3 $\beta$ -v1) was purchased from Millipore-Upstate. Additional information about the above constructs can be obtained from the authors.

Human wild-type Jade-1 and Jade-1 dd were cloned into the Xho I site of the pCS2+ vector for *Xenopus* experiments. Human *VHL* wild-type and *VHL* del96-122 were

cloned into pCS2MT+ at the Eco RI and Xba I sites. *Jade-1* shRNA plasmid was generated by targeting *Jade-1* coding sequence from nucleotide 1363 to 1385 (5'-AAGTTGAAGAGGAAGGTCAACTT -3') using a duplex oligonucleotide synthesized by OligoEngine 5'-GATCCCCGTTGAAGAGGAAGGTCAACTTCAAGAGAGTTGACCTTCCTCTTCAACTTT TTA -3' and 5'-

AGCTTAAAAAGTTGAAGAGGAAGGTCAACTCTCTTGAAGTTGACCTTCCTCTTCAAC GGG-3'. The duplex oligonucleotide was cloned into the pSuper vector (OligoEngine) using Bgl II and Hind III sites. The *Jade-1* silencing system in GIPZ shRNAmir lentiviral vector was purchased from Open Biosystems. The two silencing constructs target different parts of the *Jade-1* 3' untranslated region.

J1Sh1: Targeting exclusively the *Jade-1* short version, nucleotide 3043-3063

TGCTGTTGACAGTGAGCGCGCGTAGAAGTGAAAGTCTTATAGTGAAGCCACAGAT  
GTATAAGACTTTCACTTCTACGCCATGCCTACTGCCTCGGA

J1sh2: Targeting exclusively the *Jade-1* short version, nucleotide 1937-1957

TGCTGTTGACAGTGAGCGAGCTGGTAAACTCATTGTACATTAGTGAAGCCACAGAT  
GTAATGTACAATGAGTTTACCAGCCTGCCTACTGCCTCGGA

**Antibodies.** Mouse monoclonal  $\beta$ -catenin, E-cadherin and pVHL antibodies were from BD Transduction Laboratories. Mouse monoclonal Myc-tag, N-cadherin and polyclonal  $\beta$ -catenin against a C-terminal antigen, polyclonal GSK-3 $\beta$  and phospho- $\beta$ -catenin (detecting phosphorylated serine 33, 37 and threonine 41) antibodies were from Cell Signaling Technologies. Polyclonal Axin2 and LEF1 antibodies were from Cell Signaling Technologies. Monoclonal ubiquitin,  $\beta$ -actin,  $\alpha$ -tubulin and Flag-tag antibodies were from Sigma. Rabbit polyclonal fibrillarlin antibody was from Abcam. Polyclonal *Jade-1* antibody

has been described<sup>3</sup>. Polyclonal pVHL (FL181) antibody from Santa Cruz Biotechnology was used for pVHL immunoprecipitation and immunoblotting<sup>17</sup>. Immunoprecipitated pVHL was detected using a secondary antibody that detects only intact immunoglobulin (Sigma, Clone RG-16). Mouse monoclonal antibody for endogenous c-Myc (sc-40) was from Santa Cruz Biotechnology. Mouse monoclonal cyclin D1 antibody was from Neomarker. Goat anti-mouse and anti-rabbit HRP conjugated secondary antibodies were from Bio-Rad for immunofluorescence. Alexa Fluor 594 donkey anti-mouse and Oregon green 488 goat anti-rabbit as secondary antibodies were obtained from Invitrogen-Molecular Probes.

**Yeast two-hybrid screen.** An adult human kidney cDNA library in pB42AD (Clontech) was screened against human Jade-1 in the LexA-expressing, inducible yeast expression vector pGilda (Clontech) per manufacturer instructions. Full-length Jade-1 and other truncations of Jade-1, such as Jade-1 del1, del2, dd and dC were cloned into pGilda vector using Eco RI and Sal I sites<sup>3,8</sup>. Only Jade-1 dd did not autoactivate transcription. Therefore, Jade-1 dd was used as bait. Two x 10<sup>7</sup> pB42AD library clones were initially screened by growth in deficient medium and X-gal staining. Positive clones were rescued using the Zymoprep kit (Zymo Research) per manufacturer instructions. Nine strong candidate interactors were isolated, including  $\beta$ -catenin.

**Immunoblotting and immunoprecipitation.** Cells were lysed in 50 mM Tris-HCl, pH 7.6, 150 mM NaCl, 30 mM EDTA, 0.5% Triton X-100 with complete protease inhibitor (Roche). Immunoblotting and immunoprecipitation were performed as described previously<sup>3</sup>.

**Immunofluorescence.** Cells were grown in Chamber slides (Lab-Tek) and fixed with HEPES 20 mM, pH 7.4, NaCl 140 mM, CaCl<sub>2</sub> 2 mM, MgCl<sub>2</sub> 2 mM with 2% formaldehyde and 0.2% glutaraldehyde for 15 min. Slides were blocked with 1% BSA in PBS and 0.2% Triton X-100. Cells were incubated with primary antibody and washed with PBS. Slides were blocked in 1% BSA, 0.2% Triton X-100 in PBS, then incubated with secondary antibody. Slides were washed with PBS, mounted with Gelvatol and evaluated by fluorescence microscopy followed by confocal laser scanning microscopy (Perkin-Elmer Ultraview). As controls, one set of slides was incubated with primary antibody alone and another set with secondary antibody alone.

Co-localization was performed in cells having comparable expression of the endogenous proteins. All cells were screened. Randomly selected representative cells were analyzed. At least 15 confocal images comprising one Z-stack were generated for each cell, and co-localization was performed using the entire Z-stack. Images were background subtracted from a randomly chosen region of interest. For the endogenous proteins, the profile plots were generated using NIH ImageJ 1.37a WCIF. For over-expressed Jade-1 and  $\beta$ -catenin, randomly selected cells having comparable expression of both the constructs were screened. Randomly selected cells were used for confocal analysis. Images were background subtracted from a randomly chosen region of interest. The scatter frequency plots representing the grade of co-localization were generated with NIH ImageJ 1.37a WCIF.

**Cellular fractionation.** Cells were Dounce (Kontes) homogenized in 250 mM sucrose, 10 mM HEPES, pH 7.4, 2.5 mM MgCl<sub>2</sub>, 0.5 mM EDTA, 100  $\mu$ M Na<sub>3</sub>VO<sub>4</sub>, 100  $\mu$ M PMSF and complete protease inhibitor (Roche). After two centrifugations at 1,000 x *g* for 10 min at 4 °C, the anucleated supernatant was centrifuged at 100,000 x *g* at 4 °C for 30 min. The supernatant (S100 soluble fraction) was removed. The nuclear pellet from the first

spin was resuspended in 50 mM HEPES, pH 7.4, 50 mM KCl, 300 mM NaCl, 0.1 mM EDTA, 100  $\mu$ M  $\text{Na}_3\text{VO}_4$ , 100  $\mu$ M PMSF and complete protease inhibitor (Roche) and lysed by three cycles of freeze and thaw. The nuclear fraction was cleared by centrifugation.

**Digitonin extraction.** Cells washed with ice-cold PBS were covered with buffer containing 120 mM KCl, 5 mM  $\text{KH}_2\text{PO}_4$ , 10 mM HEPES, pH 7.4, 2 mM EGTA, 0.15 mg/ml digitonin (Sigma) and gently rocked on ice for 15 min. The gently aspirated supernatant was labeled as digitonin extract. The remaining cells were scraped from the dish and lysed for 30 min on ice in RIPA buffer containing 50 mM Tris-HCl, pH 7.4, 150 mM NaCl, 1% NP-40, 0.5% sodium deoxycholate, 0.1% SDS and 5 mM EDTA. The supernatant was obtained after centrifugation for 30 min at 4 °C.

**Generation of *Jade-1* silenced cell lines.** Lentiviral constructs were co-transfected in 293T packaging cells along with packaging, envelope and Rev vectors using Lipofectamine 2000 per manufacturer instructions. Medium containing active viral particle collected after 48 h was centrifuged and stored at -80 °C. For lentiviral infection, the cells were seeded at 50-60% confluence. The cells were treated overnight with the medium containing active viral particles along with hexadimethrine bromide (Sigma), a cationic polymer, to increase the efficiency of infection. Puromycin (Sigma) selection was initiated after 24 h. The cells were harvested after 4 days to examine the effect on Jade-1 protein.

**GST purification.** BL21 chemically competent *E. coli* (Invitrogen) were transformed with pGEX-2T  $\beta$ -catenin or pGEX-6P-1 Jade-1 constructs. Protein expression was induced in early log state ( $\text{OD}_{600}$  of 0.6-0.8) by isopropyl- $\beta$ -D-thiogalactopyranoside (IPTG) (Invitrogen). Bacteria were lysed with lysozyme (American Bioanalytical) and 1% Triton

X-100, followed by brief sonication. GST-tagged proteins were purified by passing over a glutathione Sepharose™ 4B bead slurry (GE Healthcare).

**GST pull-down assay.** Jade-1 or  $\beta$ -catenin cleaved from GST-Jade-1 and GST- $\beta$ -catenin glutathione Sepharose™ beads using Prescission protease or thrombin (GE Healthcare), respectively, were applied to GST- $\beta$ -catenin or GST-Jade-1 containing glutathione Sepharose™ beads for 2 h at 4 °C in 50 mM Tris-HCl, pH 7.6, 150 mM NaCl, 30 mM EDTA, 0.5% Triton X-100. Beads extensively washed with the same buffer containing 300 mM NaCl were boiled in Laemmli buffer (Boston Bioproducts).

***In vitro* phosphorylation of  $\beta$ -catenin.** GST- $\beta$ -catenin beads washed twice with kinase buffer containing 25 mM HEPES, pH 7.4, 10 mM MgCl<sub>2</sub>, 1 mM EDTA and 0.1 M DTT. Then GST- $\beta$ -catenin beads suspended in kinase buffer were incubated with 1 mM ATP (Sigma) and 1 unit of recombinant CK1 and GSK-3 $\beta$  (New England Biolabs) for 30 mins at 30 °C.

**Tcf/ $\beta$ -catenin-responsive luciferase reporter assay.** The 293T cells seeded in 6-well plates were cotransfected with the TOP-Flash or FOP-Flash constructs (0.6  $\mu$ g), Flag-tagged Jade-1 (full-length or dd) (1.5  $\mu$ g),  $\beta$ -catenin (wild-type or S33A) (1.5  $\mu$ g) and pRL-SV40 Renilla luciferase vector (5 ng) (to normalize for transfection efficiency) using Lipofectamine 2000 per manufacturer instructions (Invitrogen). After 48 h of transfection, luciferase assays were performed using the Dual Luciferase kit® (Promega).

***In vivo* ubiquitination assay.** The 293T cells were transiently transfected and treated with 10  $\mu$ M proteasome inhibitor MG132 (Boston Biochem) for 10-12 h before harvesting in lysis buffer containing 50 mM Tris-HCl, pH 7.6, 150 mM NaCl, 30 mM EDTA, 0.5% Triton X-100 with complete protease inhibitor (Roche). For immunoprecipitation, cell lysates were mixed with 1  $\mu$ g  $\beta$ -catenin antibody overnight at 4 °C. Protein complexes were pelleted with protein A-agarose beads (Santa Cruz), washed



in lysis buffer, eluted with Laemmli buffer (Boston Bioproducts), separated by SDS-PAGE and immunoblotted. Thirty  $\mu\text{g}$  cell extracts (5%) were probed to determine inputs.

***Ex vivo* ubiquitination of  $\beta$ -catenin using HeLa cell S100 fraction.** A HeLa S100 Conjugation kit (Boston Biochem) was used per manufacturer instructions. Briefly, 2.8  $\mu\text{M}$  GST- $\beta$ -catenin on glutathione-Sepharose<sup>TM</sup> beads was incubated with 200  $\mu\text{g}$  HeLa S100 fraction (pretreated with 200  $\mu\text{M}$  MG132 and 100  $\mu\text{M}$  ubiquitin aldehyde for 15 min at RT), 750 nM Jade-1, 600  $\mu\text{M}$  Myc-tagged ubiquitin and 5  $\mu\text{l}$  of energy regenerating solution (ERS) in 50 mM HEPES, pH 7.6, for 90 min at 37 °C.  $\beta$ -catenin ubiquitination was detected by immunoblot after cleaving  $\beta$ -catenin from GST beads using 1 unit thrombin for 2 h at RT. Reactions without ubiquitin and ERS served as negative controls.

***VHL* silencing with siRNA oligonucleotide.** For *VHL* silencing, SMARTpool® *VHL* siRNA oligonucleotides (Catalog item L-003936-00-0005; Dharmacon RNAi technologies) were transfected into cultured cells per manufacturer protocol using DHARMAFECT, and cells were harvested after 72 h. The SMARTpool includes the following 4 siRNA sequences: siRNA J-003936-09: AGGCAGGCGUCGAAGAGUA; siRNA J-003936-10: CCACCCAAAUGUGCAGAAA; siRNA J-003936-11: GGAGCGCAUUGCACAUCAA; siRNA J-003936-12: CCAAUGGAUUCAUGGAGUA.

**Synthesis of capped mRNA.** The vectors were linearized with Not I restriction enzyme, treated with Proteinase K (Sigma) and extracted with phenol. Linearized plasmid DNA (1  $\mu\text{g}/\mu\text{l}$ ) in RNase-free water was used for *in vitro* capped mRNA synthesis using the mMessage mMachine® SP6 kit (Ambion) according to manufacturer instructions.